BJP British Journal of Pharmacology

DOI:10.1111/bph.12567
www.brjpharmacol.org

RESEARCH PAPER

Changes in nerve-mediated contractility of the lower urinary tract in a mouse model of premature ageing

D Triguero, A Lafuente-Sanchis and A Garcia-Pascual

Department of Physiology, Veterinary School, Complutense University, Madrid, Spain

Correspondence
Domingo Triguero, Department of Physiology, Veterinary School, Complutense University, Avda. Puerta de Hierro s/n, 28040 Madrid, Spain. E-mail: dtriguer@ucm.es

Keywords
ageing; SAMP8 mouse; bladder; urethra; cholinergic; adrenergic; nitrergic; nerve-mediated contractility; bladder hyperactivity

Received
3 July 2013
Revised
4 December 2013
Accepted
12 December 2013

BACKGROUND AND PURPOSE
A high incidence of lower urinary tract disorders is associated with ageing. In the senescent-accelerated prone (SAMP8) mouse strain and the senescent-accelerated resistant (SAMR1) strain, we compared smooth muscle contractility in responses to intrinsic neurotransmitters, both in the bladder and urethra.

EXPERIMENTAL APPROACH
We analysed micturition frequency, the changes in muscle tension induced by electrical field stimulation or agonist administration, the density of nerves (adrenergic, cholinergic and nitrergic) and interstitial cells (ICs), as well as cGMP accumulation in bladder and urethral preparations.

KEY RESULTS
Senescent mice of the SAMP8 strain displayed increased micturition frequency and excitatory contractility of neurogenic origin in the bladder. While cholinergic nerve density remained unchanged, there was a mild sensitization to ACh in male mice. Potentiation in the detrusor may be also provoked by the stronger contribution of ATP, together with reduced adrenergic innervation in males and COX-derived prostanoid production in females. The greater excitatory contractility in the urethra was probably due to the sensitization to noradrenaline, in conjunction with attenuated nitrergic relaxation. There were also fewer neuronal NOS immunoreactive (ir) nerves and vimentin-positive ICs, although the sildenafil- and diethylamine-NONOate-induced relaxations and cGMP-ir remained unchanged.

CONCLUSIONS AND IMPLICATIONS
Premature senescent mice exhibit bladder and urethral hyperexcitability, coupled with reduced urethral relaxation of neurogenic origin, which could model the impaired urinary function in elderly humans. We propose that senescence-accelerated mice provide a useful tool to analyse the basic mechanisms of age-related changes in bladder and urethral function.

Abbreviations
AVP, arginine-vasopressin; DEA/NO, diethylamine-NONOate; EFS, electrical field stimulation; HE, haematoxylin-eosin; IC, interstitial cell; ir, immunoreactive or immunoreactivity; L-NOARG, N^G-nitro-L-arginine; LUT, lower urinary tract; nNOS, neuronal NOS; ODQ, 1H-[1,2,4]oxadiazolo[4,3-a]quinoxalin-1-one; SAMP8, senescence-accelerated mouse prone; SAMR1, senescence-accelerated mouse resistant; TTX, tetrodotoxin; VAChT, vesicular ACh transporter; αβ-MeATP, αβ-methylene-ATP

Introduction

Due to the dramatic increase in life expectancy, ageing represents a major medical challenge with significant socio-economic implications. In contrast to cardiovascular, neurological and rheumatic diseases, disorders affecting the lower urinary tract (LUT) are not considered as a significant threat to health, despite their high prevalence and deleterious effects on quality of life. Indeed, symptoms of LUT disorders were reported to be close to 95% of the population aged over 60 in an online survey of 30 000 patients in the USA, UK and Sweden (Coyne *et al.*, 2009). Furthermore, the premature onset of this condition (in some individuals in as early as their mid-40s; Wagg and Cohen, 2002) suggests that most individuals affected will suffer from LUT disorders for 25–40 years. However, current data on LUT disorders in ageing are extremely variable (Michel and Barendrecht, 2008). Despite their considerable size, the human cohorts are highly heterogeneous (Irwin *et al.*, 2006; Coyne *et al.*, 2009), and the presence of concurrent pathologies, such as hypercholesterolemia, vascular or connective tissue disorders (Roosen *et al.*, 2009), is superimposed upon the primary degenerative changes common to ageing. Significantly, such heterogeneity has also been reported in animals (Lluel *et al.*, 2003; Lagou *et al.*, 2006; Zhao *et al.*, 2010).

Mouse models have been developed that spontaneously show accelerated senescence (Takeda *et al.*, 1981), such as the senescence-accelerated mouse prone strain (SAMP) and they have been used to study the effects of ageing on the nervous, cardiovascular and endocrine systems (Ueno *et al.*, 2001; Forman *et al.*, 2011). Mice from the same originator strain but with a normal life expectancy (senescence-accelerated mouse resistant; SAMR1) serve as controls (Takeda *et al.*, 1981). SAMP strains have been shown to develop age-associated degenerative disorders, including senile osteoporosis, articular degenerative changes, deficits in learning and memory, presbycusis, retinal atrophy, systemic amyloidosis and immune impairment (Takeda *et al.*, 1997). However, LUT disorders in this model of ageing have yet to be described.

Accordingly, the main goal of the present study was to characterize the differences in LUT contractility between SAMP8 and SAMR1 mice. To achieve this, we carried out a comparative study between different regions of the bladder (dome, detrusor and trigone) from young and aged mice of both sexes, as well as on the female urethra (proximal, medial and distal). In these animals, we first analysed micturition frequency, as well as the changes in contractile and relaxant responses induced by nerve stimulation or agonists. Using immunohistofluorescence, we also assessed the density of the main excitatory (cholinergic and adrenergic) and inhibitory (nitrergic) nerves and interstitial cells (ICs) in these mice, as well as the accumulation of cGMP. The physiological changes we have identified could serve as a useful model of those factors that have an important influence on urinary function in elderly humans.

Methods

All animal care and experimental procedures complied with the European Guidelines Council Directive 2010/63/EU and were approved by the Ethical Committee of the Complutense University. All studies involving animals are reported in accordance with the ARRIVE guidelines for reporting experiments involving animals (Kilkenny *et al.*, 2010; McGrath *et al.*, 2010). A total of 166 animals were used in the experiments described here. The LUT was isolated from male and female SAMP8 and SAMR1 mice (36–38 weeks old, 31–38 g, n = 38–45 per group). These mice were bred from founders provided by Dr JAF Tresguerres (Physiology Department at the Complutense University Medical School, Madrid, Spain), and the mice were housed on a 12/12 h light/dark cycle with *ad libitum* access to food and water.

Voiding frequency

Micturition frequency was measured as described previously (Dickson *et al.*, 2006) and at the same time of the day (early morning). Water was withdrawn 1 h before placing the mice in cages lined with filter paper for 60 min. The total number of urine spots, as well as the subset of small diameter spots (<0.5 cm), were counted and expressed as the number of voids per hour.

Recording of isometric tension

The mice were killed by cervical dislocation, the entire LUT removed and placed in cold (4°C) Krebs solution (in mM): 119 NaCl, 4.6 KCl, 1.5 $CaCl_2$, 1.2 $MgCl_2$, 15 $NaHCO_3$, 1.2 KH_2PO_4, 0.01 EDTA and 11 glucose. The bladder and urethra were dissected out, and stripped of fat and connective tissue, and longitudinal strips (3–4 mm long) were obtained from the lateral detrusor. The female urethra was opened longitudinally, removing the external urethral sphincter to obtain a longitudinal 3–4 mm long strips.

Preparations were mounted in 5 mL organ baths containing Krebs solution (37°C) bubbled with 95% O_2 and 5% CO_2 (pH 7.4). The isometric tension was recorded using Grass FT03C transducers (Grass Instruments, Quincy, MA, USA) and it was displayed on a Macintosh computer using a MacLab analogue-to-digital converter v5.5 (AD Instruments Ltd, Hastings, East Sussex, UK).

In preliminary experiments, the optimal length (L_0) for force development was established through the length–force relationship. The passive tension near L_0 that produced maximal active responses was 4.12 ± 0.77 mN (n = 7) for the female detrusor and 6.91 ± 0.12 mN (n = 7) for the male, and it was 1.73 ± 0.53 mN (n = 7) for the urethra. In subsequent experiments, preparations were equilibrated for 60 min at a resting tension of 4 mN (female detrusor), 7 mN (male detrusor) and 2 mN (urethra), and tissue viability was tested by exposure to high [K^+] (120 mM). Electrical field stimulation (EFS) was achieved using a Grass S-48 stimulator (Grass Instruments) connected to platinum electrodes that were placed parallel to the preparation and coupled to a stimulus splitter (Med-Lab Instruments, Loveland, CO, USA). Square-wave pulses of 0.8 ms were delivered at 2 min intervals with a supra-maximal voltage (current strength, 200 mA), a train duration of 5 s and at frequencies ranging from 1 to 50 Hz.

Contractions induced by EFS (1–50 Hz) were assessed in urethral and bladder preparations at basal tension, and they were compared with those induced by the cumulative addition (10^{-8} to 10^{-2} M) of noradrenaline, ACh or ATP. Urethral

contractions were induced by EFS in the presence of both the NOS inhibitor N^G-nitro-L-arginine (L-NOARG; 0.1 mM; see Alexander *et al.*, 2013a for target information) to prevent the release of NO from nerves, and D-tubocurarine (0.1 μM) to prevent the stimulation of somatic innervation of the urethral-striated muscle (see Alexander *et al.*, 2013b). To determine the involvement of ACh, ATP and prostanoids in EFS-induced detrusor contractions, atropine (1 μM), αβ-methylene-ATP (αβ-MeATP; 100 μM) and indomethacin (30 μM) were added consecutively 30 min before a second frequency–response curve was constructed. In addition, phentolamine (0.1 mM) was used to determine the involvement of noradrenaline in the EFS-induced urethral contractions (see Alexander *et al.*, 2013c) . Urethral relaxations of nitrergic origin were achieved by EFS preparations that were pre-contracted with a submaximal concentration of arginine-vasopressin (AVP, 0.1 μM) in the continued presence of atropine (1 μM) and guanethidine (50 μM) to avoid cholinergic and adrenergic excitatory influences, respectively, and D-tubocurarine (10 μM) to block the nicotinic activation of the striated urethral sphincter. The concentration–response relaxation curves induced by the NO donor diethylamine-NONOate (DEA/NO; 10^{-8} to 10^{-2} M) or the PDE5 inhibitor sildenafil (10^{-8} to 10^{-3} M) were also tested in AVP pre-contracted preparations. After washing, some preparations were pretreated for 30 min with the NOS inhibitor L^G-nitro-L-arginine (L-NOARG; 0.1 mM) or the GC inhibitor 1H-[1,2,4]oxadiazolo[4,3-a]quinoxalin-1-one (ODQ; 0.1 mM) before subjecting them to another contraction (AVP)–relaxation (EFS, DEA/NO or sildenafil) protocol in the continued presence of the inhibitor. The neural dependency of EFS-mediated responses was tested by finally adding tetrodotoxin (TTX; 1 μM). In all the experiments, parallel preparations receiving only the solvent for the different drugs were used as controls.

Immunohistofluorescence

Animals were anaesthetized (100 mg·kg^{-1} ketamine + 10 mg·kg^{-1} xylazine, i.p.) and perfused through the heart for 30 min with heparinized (600 IU·L^{-1}) 0.1 M phosphate buffer (PB; Na_2HPO_4 57.7 mM, NaH_2PO_4 42.3 mM, pH 7.0), followed by 4% paraformaldehyde in PB. The LUT was removed, and the bladder and female urethra were prepared as whole-mount preparations (~100 μm thick). The muscle layer was separated from the lamina propria and pinned to a Sylgard base for 30 min in ice-cold 4% paraformaldehyde in 0.1 M PB. Fixed tissues were cryoprotected with increasing concentrations of sucrose in ice-cold 4% paraformaldehyde (10% for 90 min followed by 20% for 120 min), incubated overnight at 4°C in 30% sucrose in PB, snap-frozen in liquid nitrogen-cooled isopentane and stored at –80°C for 15 days.

The urethral preparations in which immunoreactive (ir) cGMP was assessed were first studied in functional experiments, facilitating direct comparison between relaxation and cGMP accumulation. AVP pre-contracted preparations were exposed to the PDE inhibitors IBMX (1 mM) and zaprinast (0.1 mM) to prevent cGMP breakdown, both 30 s prior to stimulation and throughout the experiment. This allowed sufficient accumulation of cGMP to be visualized by immunofluorescence (Garcia-Pascual *et al.*, 2008). Tissues were stimulated by DEA/NO (0.1 mM) or sustained EFS (4 Hz) for 4 min, with the control preparations processed identically but without exposing them to DEA/NO or EFS. Some preparations were pretreated with L-NOARG (0.1 mM) or ODQ (0.1 mM) for 30 min to assess the specificity of the reaction. Experiments were terminated by snap-freezing with liquid nitrogen and the tissue was immediately processed for immunofluorescence, as described elsewhere (Garcia-Pascual *et al.*, 2008).

Briefly, after washing with PB (3 × 5 min), preparations were blocked for 30 min with a 3% solution of normal donkey serum (Chemicon International, Temecula, CA, USA) containing 0.3% Triton X-100. The tissue was then exposed to the primary antibody (or antibodies for dual labelling) for 48 h of incubation at 4°C diluted in 2% donkey serum and 0.3% Triton X-100, and then to the secondary antibody for 2 h in the dark at room temperature with gentle shaking (all the antibodies used are listed in Table 1). In all cases, negative controls lacking the primary antibody were run in parallel. After washing with PB (3 × 10 min), the preparations were

Table 1

Primary and secondary antibodies used in the immunohistofluorescence studies

Antibody	Dilution source
Primary	
Rabbit anti-nNOS polyclonal antiserum (160870)	1:500 Cayman Chemical (Ann Arbor, MI, USA)
Rabbit anti-vimentin polyclonal antiserum (ab8545)	1:500 Abcam (Cambridge, UK)
Goat anti-vesicular ACh transporter polyclonal antiserum (ab34852)	1:200 Abcam
Sheep anti-TH polyclonal antiserum (ab113)	1:400 Abcam
Sheep anti-cGMP polyclonal antiserum	1:2000[a]
Secondary	
Alexa 594 conjugated donkey anti-rabbit (A21207)	1:400 Molecular Probes
Alexa 488 conjugated donkey anti-sheep (A11015)	1:400 Molecular Probes
Alexa 488 conjugated donkey anti-goat (A11055)	1:400 Molecular Probes

[a]A generous gift from Professor De Vente, Maastricht University, Holland. Manufacturer catalogue numbers are between brackets.

mounted on slides with Prolong Gold® antifade reagent (Molecular Probes, Eugene, OR, USA), air-dried at room temperature for 12 h and visualized on an Axioplan 2 fluorescence microscope (Carl Zeiss Microimaging, Göttingen, Germany). Each preparation was photographed with a Spot-2 digital camera (Diagnostic Instruments, Sterling Heights, MI, USA), and the images were stored digitally as 12-bit images using MetaMorph 7.0 software (MDS Analytical Technologies, Toronto, ON, Canada) and processed using Adobe Photoshop CS 8.0.1 (San Jose, CA, USA).

Some preparations were examined by confocal laser-scanning microscopy (Leica SP2 DMIRE2, Heidelberg, Germany). The confocal micrographs shown are digital composites of Z-series scans from several optical sections through the depth of the preparation (2 µm each; Leica Confocal Software-LCS; Leica Microsystems, Barcelona, Spain).

For histological evaluation, cryostat sections (10 µm; CM1850 UV; Leica Microsystems) were obtained from detrusor preparations embedded in Tissue-Tek OCT compound. The sections were thawed onto poly-L-lysine-coated slides, air-dried at room temperature for 12–24 h and then stained with haematoxylin-eosin (HE).

Data analysis

Contractile and relaxant responses. Contractile responses were expressed as a proportion of the KCl-induced contraction (120 mM) or as a percentage of the maximum response for each preparation. Urethral relaxations were normalized to the response elicited by AVP (0.1 µM) immediately before each stimulation. In some cases, the slope of the relaxation curves induced by DEA/NO and EFS (dF/dt; speed of response) was also measured. All responses were obtained using Chart 5 software (Version 5.5.1 for Macintosh).

The EF_{50} and pD_2 values represent the frequency of stimulation and the negative logarithm of the agonist concentration required to induce 50% of the maximum response (E_{max}). Concentration–response curves were analysed using GraphPad Prism software (Version 5.0; GraphPad Software, San Diego, CA, USA), assuming a Hill coefficient =1, by fitting to a simple logistic equation of the form Y = min + (max – min)/(1 + 10^(Log EC_{50} – Log X)), where min and max were the minimum and maximal effect, The EC_{50} was the agonist concentration that elicited 50% of the maximum effect, and X was the molar concentration of the drug. Parallel preparations treated with solvent alone were used as controls.

Quantification of innervation density. Innervation density was quantified by measuring the proportion of immunoreactivity exceeding the threshold value in a selected area, as described previously (Garcia-Pascual *et al.*, 2008). Hand-drawn areas of muscle layer were analysed by the personnel at the Microscopy and Cytometry Centre (Complutense University, Madrid, Spain), without knowledge of the treatment groups. The average areas chosen were 59 375 ± 9079 µm^2 (n = 30) at 10× and 12 951 ± 2149 µm^2 (n = 27) at 20× in the bladder; and 73 291 ± 8603 µm^2 (n = 31) at 10× and 16 469 ± 1628 µm^2 (n = 29) at 20× in the urethra. For each experimental group, measurements were taken from four to five randomly selected areas of tissue per animal, and from at least four animals. Images were obtained at a constant time exposure to permit direct comparisons and a threshold was established to subtract the background staining.

Statistical analysis. The data are presented as the mean ± SE of n experiments (each experiment from a different animal). The differences between groups were assessed using one way ANOVA and the means of two experimental groups were compared using the Student's t-test (paired or unpaired). The minimum level of significance was established at $P < 0.05$ and the statistical analyses were performed using GraphPad Prism software.

Materials

ACh, ATP, atropine sulphate, [Arg^8] vasopressin acetate salt (AVP), guanethidine monosulphate, IBMX, indomethacin, αβ-MeATP, noradrenaline bitartrate, L-NOARG, phentolamine hydrochloride, D-tubocurarine hydrochloride and zaprinast were purchased from Sigma (Steinheim, Germany). DEA/NO diethylammonium salt and ODQ were purchased from Alexis Biochemicals (Lausanne, Switzerland). TTX (with citrate) was obtained from Alomone Labs (Jerusalem, Israel) and sildenafil was a gift from Pfizer (Madrid, Spain). All drugs were dissolved in distilled water except for indomethacin (in ethanol), IBMX and zaprinast (in DMSO), ODQ (in acetonitrile) and DEA/NO (in 0.01 M NaOH). The final concentration of solvents was lower than 1/1000 (v/v). Stock solutions were stored at –20°C and working dilutions were prepared in 0.9% NaCl.

Results

General and urological signs of ageing in SAMP8 mice

SAMP8 mice showed external symptoms of ageing that include decreased motility, piloerection, eye ulcers and a prominent xiphoid process. By contrast, SAMR1 animals of the same age were as healthy in appearance as young adult mice. We found 8 out of 83 SAMP8 mice to have tumours in different organs but not in the LUT, whereas no tumours were detected in any SAMR1 mice. The general macroscopic, histological and functional features of both strains are summarized in Table 2, and the only significant strain difference was the lower body weight of SAMP8 mice of both sexes. Notably, the males in both strains had significantly heavier bladders relative to body weight (Table 2). HE-stained bladder sections revealed no differences in the appearance (data not shown) and size (Table 2) of the lamina propria or the muscle layer, although cell infiltration into the lamina propria was occasionally observed in SAMP8 bladders (data not shown).

Although bladder contractions elicited with 120 mM K^+ were significantly stronger in males (consistent with their heavier bladders; Table 2), they were similar in both strains. Strain and gender differences were observed in the total and low-volume voiding frequency, being significantly higher in both male mice and in SAMP8 mice (Figure 1).

Nerve-mediated detrusor contractions

EFS-induced contractions were stronger in SAMP8 than in SAMR1 mice, producing a leftward shift in the frequency–

Table 2

Comparison of body and bladder weight, bladder layer thickness, and the magnitude of the contractile response to a high concentration of potassium in SAMP8 and SAMR1 mice

		SAMR1		SAMP8	
		♂	♀	♂	♀
Body weight (g)		38.4 ± 1.02 (*19*)	35.2 ± 0.93 (*19*)	32.0 ± 0.71 (*19*)***	30.7 ± 1.42 (*19*)**
Bladder weight (% body weight)		1.52 ± 0.14 (*19*)	0.71 ± 0.10 (*19*)†††	1.92 ± 0.23 (*19*)	0.73 ± 0.14 (*19*)†††
Layer thickness (μm)	Lamina propria	302 ± 30.2 (*5*)	296 ± 22.3 (*5*)	330 ± 40.1 (*5*)	325 ± 75.0 (*5*)
	Muscle layer	431 ± 46.3 (*5*)	406 ± 34.0 (*5*)	413 ± 35.4 (*5*)	375 ± 25.1 (*5*)
Contractile force (mN) [K^+ 120 mM]		9.61 ± 0.82 (*15*)	7.03 ± 0.82 (*15*)†††	10.8 ± 1.21 (*15*)	7.32 ± 0.73 (*15*)†††

The values represent the mean ± SE (*n*): **$P < 0.01$, ***$P < 0.001$ versus SAM-R1; †††$P < 0.001$ versus ♂ (ANOVA followed by Student's *t*-test).

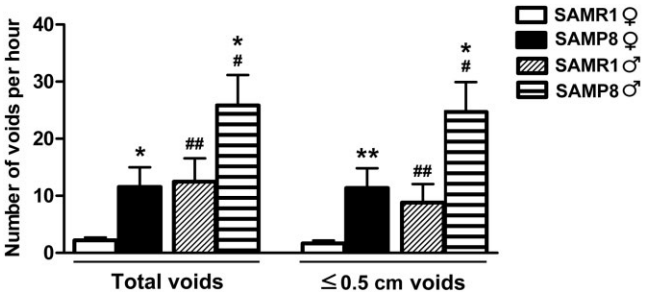

Figure 1

Voiding frequency in SAMP8 and SAMR1 mice. The total and the small volume voids (≤0.5 cm) are expressed as the number of voids per hour in male and female SAMR1 and SAMP8 mice. The data are expressed as the mean ± SE (n = 27–28 per group): *$P < 0.05$, **$P < 0.01$ versus SAMR1; #$P < 0.05$, ##$P < 0.01$ versus female (ANOVA followed by Student's *t*-test).

response curve, with significant reductions in the EF_{50} and an increase in the E_{max} (Figure 2A). Representative traces of the cumulative inhibitory effects produced in the presence of atropine (1 μM), αβ-Me ATP (100 μM) and indomethacin (30 μM) are shown (Figure 2B). When the E_{max} and EF_{50} values were expressed in relation to their own maximum value in each frequency–response curve (Table 3), it was evident that the atropine-sensitive component of the responses was more prominent in male than in female SAMR1 mice, yet not in SAMP8 animals, (Table 3). Subsequent purinergic receptor desensitization in the presence of αβ-MeATP (100 μM) reduced the atropine-resistant contractions further, and to a similar extent in both genders and in both strains (Table 3). Indomethacin (30 μM) only inhibited the responses in female SAMP8 preparations (Table 3) and the residual responses were not further reduced by TTX in any group (1 μM; data not shown)

ACh- and ATP-induced detrusor contractions

The cumulative addition of ACh and ATP (10^{-8} to 10^{-2} M) resulted in concentration-dependent phasic contractions (Figure 3). While the E_{max} values for ACh were similar in all groups [in females, 156 ± 13.5 (n = 14) in SAMR1 vs. 158 ± 10.5 (n = 17) in SAMP8; in males, 153 ± 2.51 (n = 10) in SAMR1 vs. 152 ± 2.72 (n = 19) in SAMP8], the male pD_2 values were higher in SAMP8 (5.22 ± 0.23, n = 19) than in SAMR1 preparations (3.80 ± 0.21, n = 10; $P < 0.01$; Figure 3). However, the pD_2 was not different between female SAMR1 (4.14 ± 0.22, n = 14) and SAMP8 mice (4.30 ± 0.24, n = 17; Figure 3). A maximum response could not be obtained for ATP-induced contractions and thus E_{max} values should be considered as estimates (Figure 3). SAMP8 preparations were more sensitive to ATP, particularly those from males that displayed a higher E_{max}, increasing from 43.4 (± 0.81, n = 7) for SAMR1 mice to 59.0 (±1.33, n = 13) for SAMP8 ($P < 0.001$), as well as higher pD_2 values, which augmented from 2.61 (± 0.20, n = 7) in SAMR1 to 3.23 (± 0.22, n = 13) in SAMP8 mice ($P < 0.001$; Figure 3). In females, there was also a significant increase in the pD_2 between SAMR1 (2.91 ± 0.44, n = 14) and SAMP8 mice (3.92 ± 0.21, n = 17; $P < 0.05$; Figure 3) while only a slight yet significant decrease in E_{max} was observed in SAMP8 mice [38.4 ± 3.71 (n = 14) as opposed to 30.31 ± 1.63 in SAMR1 mice (n = 17); $P < 0.05$; Figure 3].

Immunoreactivity (ir) for the vesicular ACh transporter (VAChT) and tyrosine hydroxylase (TH) in the bladder

In bladder preparations (Figure 4A and B), VAChT-ir was evident in a dense fibre network running parallel to the muscle bundles, and this was distributed evenly in all regions with no significant gender or strain differences (Figure 4E). When TH-ir was assessed, thick nerve trunks and varicose fibre networks were associated with intramural ganglia (Figure 4C and D). Marked gender and regional variability in TH-ir density were observed within the bladder, being more prominent in the trigone and in males (Figure 4F). Furthermore, TH-ir was weaker in the detrusor and trigone of male SAMP8 mice than in SAMR1 mice (Figure 4F). No VAChT-ir or TH-ir was observed in the negative controls (data not shown).

Nerve-mediated urethral contractions

Urethral contractions induced by high concentrations of K^+ were similar in both strains (0.34 ± 0.02 mN and 0.29 ± 0.04 mN in SAMR1 and SAMP8 respectively; n = 10–13). In the presence of L-NOARG (0.1 mM) and D-tubocurarine

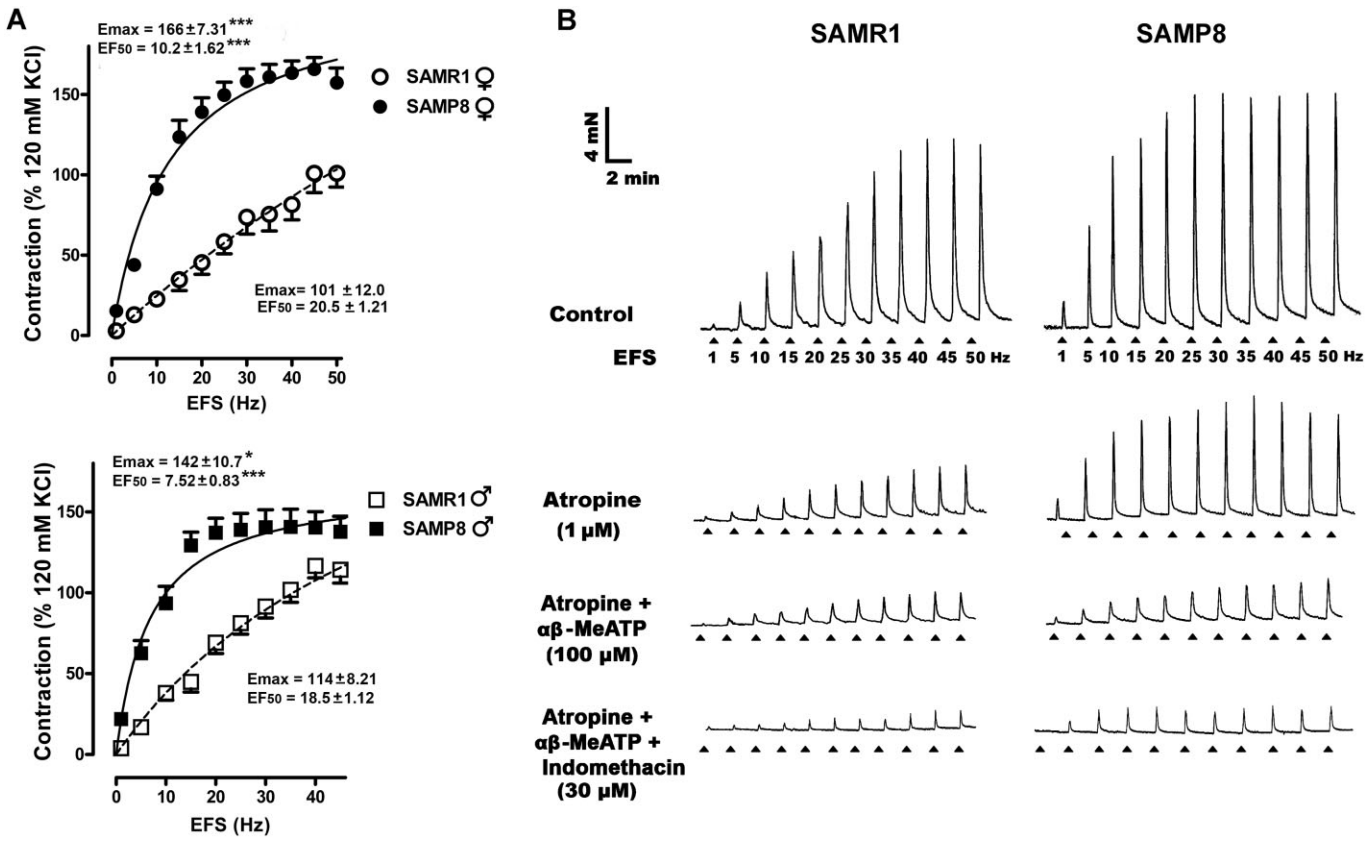

Figure 2

Frequency-dependent contractile response in the detrusor muscle of SAMP8 and SAMR1 mice. (A) Frequency–response curves in female (*top*) and male (*bottom*) SAMR1 or SAMP8 detrusor muscles. The data represent the contraction relative to that induced by 120 mM KCl (mean ± SE, n = 10–14). The E_{max} and EF_{50} values obtained from the respective curves are included in the figure: *P < 0.05; ***P < 0.001 versus SAMR1. (B) Representative traces for male SAMR1 (*left*) and SAMP8 (*right*) mice in which detrusor contractions were elicited by EFS (5 s, 1–50 Hz) under control conditions (*top*) and after 30 min of cumulative incubations with atropine (1 μM), αβ-MeATP (100 μM) and indomethacin (30 μM, *bottom*).

(0.1 μM), EFS (1–50 Hz) elicited transient biphasic contractions that consisted of a fast component, followed by a slower contraction that remained almost constant across the entire range of frequencies (Figure 5A). Fast contractions were frequency-dependent, reaching the maximum response (E_{max}) at approximately 50 Hz in SAMR1 animals, whereas a true maximum could not be attained in SAMP8 preparations (Figure 5A). Similar EF_{50} values were obtained in both strains, although the E_{max} was significantly higher in SAMP8 (Table 4). Blocking α-adrenoceptors with phentolamine (0.1 mM) reduced the E_{max} in both strains, although these residual contractions were not further reduced by TTX (1 μM; Table 4).

Noradrenaline-induced urethral contractions

The cumulative addition of noradrenaline (10^{-8} to 10^{-2} M) induced concentration-dependent contractions in urethral preparations that were significantly more pronounced in aged animals at the highest concentrations used (E_{max}). The pD_2 values were similar in both strains consistent with those observed in the EFS-induced responses (Figure 5B; Table 4).

VAChT-ir and TH-ir in the urethra

In the urethral muscle layer, VAChT-ir was found in varicose fibre networks and intramural ganglia (Figure 6A and B), with a similar density in all the regions examined (proximal, medial and distal) in both strains (Figure 6E). The urethral TH-ir network was denser than the VAChT-ir one, and consisted of thin nerve endings running parallel to the muscle bundles (Figure 6C) and intramural TH-ir ganglia (Figure 6D). Similarly, TH-ir was distributed uniformly in all urethral regions in both strains (Figure 6E). VAChT-ir or TSH-ir was not detected in the absence of the corresponding primary antibodies (data not shown).

nNOS-ir in the bladder and urethra

When we considered nNOS-ir, significant regional and gender differences were evident in the muscle layers of the bladder and urethra from SAMR1 and SAMP8 mice (Figure 7). In both males and females, nNOS-ir was scarce in the bladder dome, becoming progressively denser towards the trigone and urethra (Figure 7J and K). Thick nerve trunks with small and scattered ganglion cells predominated in the bladder trigone (Figure 7A–D), as well as large intramural ganglia (Figure 7E). The density of nNOS-ir was significantly lower in the whole bladder of females than males (Figure 7J and K). While no strain differences were observed in female bladders (Figure 7J), nNOS-ir was significantly lower in the male

Table 3

EF_{50} and E_{max} values obtained from the frequency–response contraction curves of SAMR1 and SAMP8 detrusor muscle under different conditions

	SAM-R1			SAM-P8		
♀	EF_{50}	E_{max} (% maximum)	*n*	EF_{50}	E_{max} (% maximum)	*n*
Control	18.3 ± 2.15	94.6 ± 1.45 (45 Hz)	12	9.7 ± 0.72***	97.1 ± 1.22 (25–30 Hz)	14
Atropine (1 μM)	16.1 ± 1.28	53.4 ± 4.73$^{\#\#\#,\dagger\dagger\dagger}$	11	7.0 ± 0.47***	56.2 ± 7.21†††	9
Atropine + αβ-MeATP (100 μM)	18.8 ± 2.95	21.2 ± 2.24$^{\Phi\Phi}$	10	6.64 ± 0.95**	28.3 ± 3.24$^{\Phi\Phi\Phi}$	9
Atropine + αβ-MeATP + Indomethacin (30 μM)	13.6 ± 1.51	15.8 ± 5.66	6	12.5 ± 0.61	11.3 ± 3.73$^{\Delta}$	6
	SAM-R1			**SAM-P8**		
♂	EF_{50}	E_{max} (40 Hz)	*n*	EF_{50}	E_{max} (20–25 Hz)	*n*
Control	16.5 ± 1.34	94.4 ± 1.56 (40 Hz)	13	7.53 ± 0.86***	97.6 ± 1.77 (20–25 Hz)	10
Atropine (1 μM)	12.9 ± 0.86	27.8 ± 1.98††	7	6.04 ± 0.53***	49.2 ± 8.72*†††	7
Atropine + αβ-MeATP (100 μM)	13.1 ± 1.87	15.2 ± 1.77$^{\Phi}$	6	9.02 ± 1.28	17.1 ± 4.25$^{\Phi\Phi}$	6
Atropine + αβ-MeATP + Indomethacin (30 μM)	13.2 ± 1.59	10.0 ± 1.23	6	15.3 ± 5.04	11.5 ± 2.34	6

E_{max} (maximum response) values are expressed relative to the maximum response in each frequency–response curve and the EF_{50} represents the negative logarithm of the frequency that produces 50% of that maximum. The frequency at which the maximum was obtained is shown in brackets. The EF_{50} and E_{max} are expressed as the mean ± SE: $^{\dagger\dagger}P < 0.01$, $^{\dagger\dagger\dagger}P < 0.001$ versus the control group; $^{\Phi}P < 0.05$, $^{\Phi\Phi}P < 0.01$, $^{\Phi\Phi\Phi}P < 0.001$ versus the atropine-treated group; $^{\Delta}P < 0.05$ versus the atropine + αβ-MeATP-treated group (paired *t*-test, comparisons made in absolute values); $^{*}P < 0.05$, $^{**}P < 0.01$, $^{***}P < 0.001$ versus SAMR1; $^{\#\#\#}P < 0.001$ versus male (ANOVA followed by unpaired *t*-test, comparisons made in normalized values).

Table 4

The EF_{50}, pD_2 and E_{max} values obtained from the contractile frequency–response curve and the noradrenaline induced concentration–response curve in SAMR1 and SAMP8 urethras

	SAMR1			SAMP8		
	EF_{50}	E_{max} (% KCl)	*n*	EF_{50}	E_{max} (% KCl)	*n*
Control	23.6 ± 3.40	55.9 ± 4.41	10	28.6 ± 2.12	94.7 ± 12.5*	13
Phentolamine (0.1 mM)	18.8 ± 2.91	22.3 ± 3.42$^{\#\#}$	9	24.7 ± 1.90	43.4 ± 6.10$^{\#\#}$*	10
TTX (1 μM)	21.3 ± 3.10	17.5 ± 4.53$^{\#\#}$	7	19.9 ± 1.90	35.6 ± 8.73$^{\#\#}$*	6
	pD_2	E_{max} (% KCl)	*n*	pD_2	E_{max} (% KCl)	*N*
Noradrenaline	5.41 ± 0.42	76.1 ± 7.31	10	5.7 ± 0.23	117 ± 11.7*	11

E_{max} (maximum responses) is expressed relative to the contraction induced by 120 mM KCl, and the EF_{50} and pD_2 represent the negative logarithm of the frequency or agonist concentration that induces 50% of the maximum response respectively. The E_{max}, EF_{50} and pD_2 are expressed as the mean ± SE: $^{*}P < 0.05$ versus SAMR1; $^{\#\#}P < 0.01$ versus control group (ANOVA followed by Student's *t*-test; $n = 6–13$).

detrusor and trigone of the SAMP8 mice (Figure 7K). In the female urethra, a dense network of thin nNOS-ir fibres and intramural ganglia was observed (Figure 7F–I), although this immunoreactivity was significantly weaker in the proximal and medial urethra of SAMP8 mice (Figure 7J).

Double labelling for nNOS and VAChT revealed these fibre networks co-localized to a large extent in the urethra (Figure 8A–C). However, double labelling for nNOS and TH showed that nitrergic and adrenergic nerves ran in close proximity, occasionally establishing close contacts that could be discerned by confocal microscopy (Figure 8D–F).

Urethral relaxations induced by nitrergic EFS and the addition of exogenous agonists

In the presence of atropine (1 μM), guanethidine (50 μM) and D-tubocurarine (10 μM), AVP (0.1 μM) induced stable contractions that reached 590 ± 62% ($n = 30$) of the 120 mM KCl-induced response in preparations from SAMR1 mice and 700 ± 83% ($n = 30$) in SAMP8 urethras. EFS elicited frequency-dependent relaxations of nitrergic origin in pre-contracted preparations, relaxation that was blocked in the presence of L-NOARG (0.1 Mm; Figure 9A). These frequency-dependent

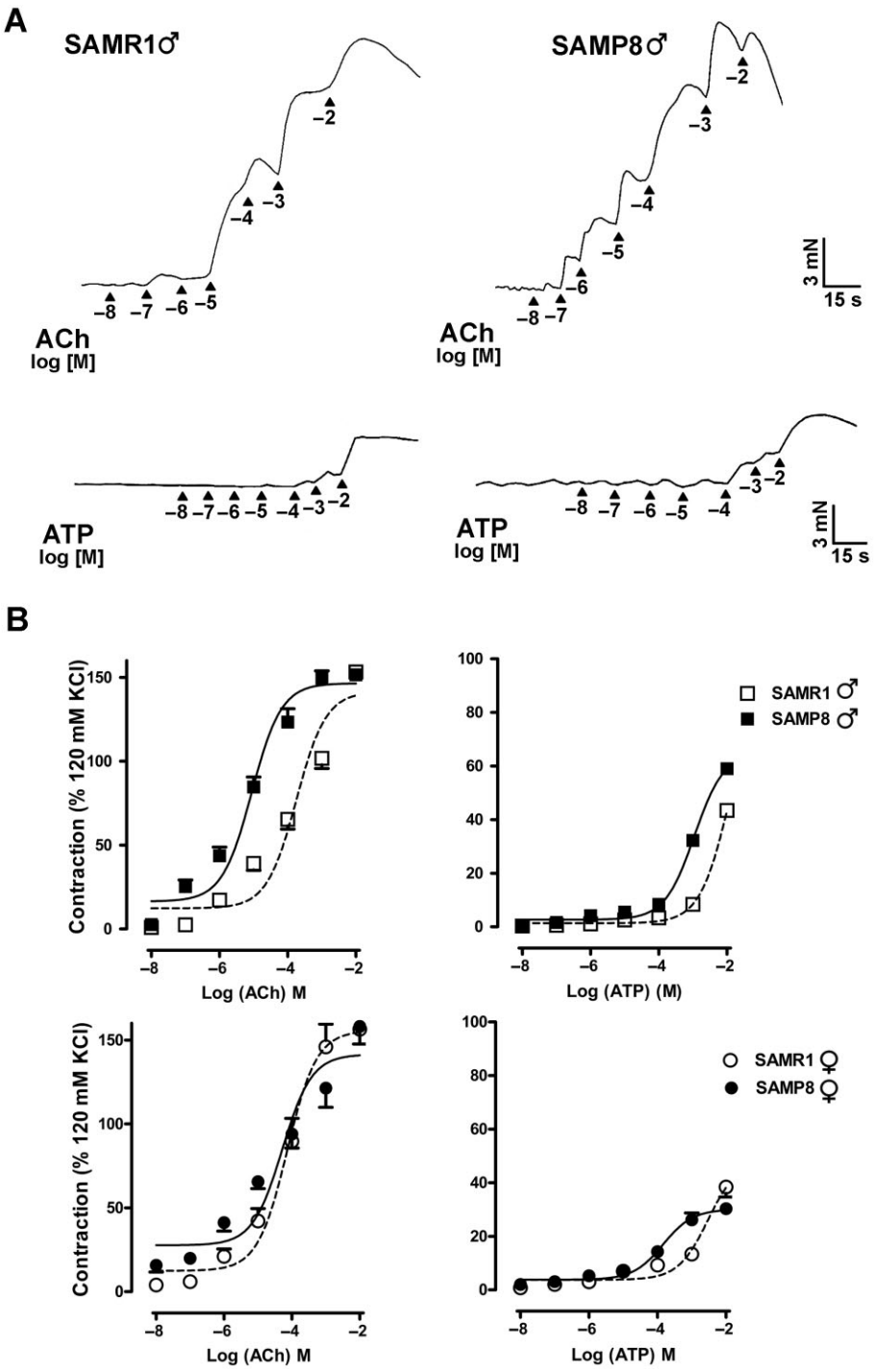

Figure 3

Concentration-dependent contractions induced by ACh and ATP in the SAMR1 and SAMP8 detrusor muscle. (A) Representative traces for male SAMR1 and SAMP8 mice in which detrusor contractions were elicited by exogenous addition of cumulative concentrations of ACh (*top*) and ATP (*bottom*). (B) Response of female (*top*) and male (*bottom*) SAMR1 or SAMP8 detrusor muscles to ACh (*left*) and ATP (*right*). The data represent the contraction relative to that induced by 120 mM KCl (mean ± SE, n = 10–19).

relaxations were significantly lower in tissue from SAMP8, compared with that from SAMR1 mice (Figure 9B). Cumulative addition of DEA/NO (10^{-8} to 10^{-2} M) or sildenafil (10^{-8} to 10^{-2} M) induced comparable concentration-dependent urethral relaxations in both strains (Table 5). Pre-incubation with ODQ (0.1 mM) significantly reduced the pD_2 values in all cases, confirming their dependence on cGMP formation (Table 5).

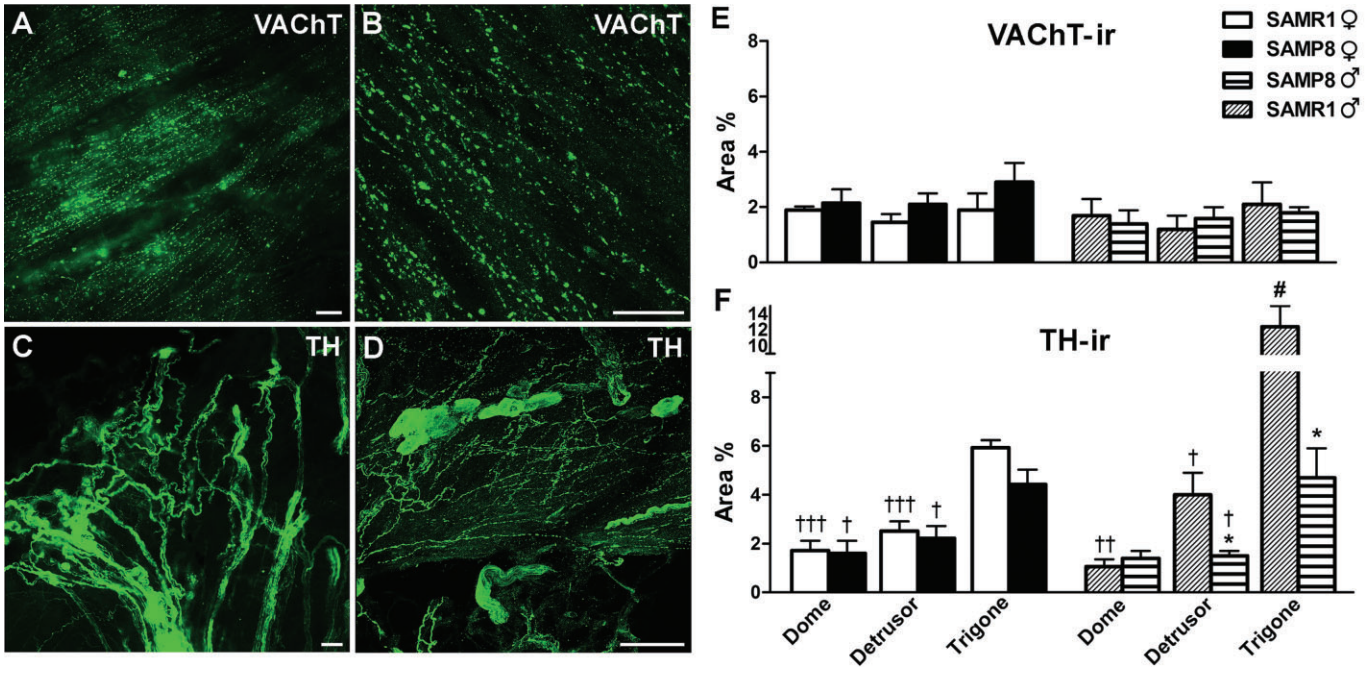

Figure 4

VAChT- and TH-ir in SAMR1 and SAMP8 bladders. (A) Abundant VAChT-ir cholinergic nerves are evident in the male SAMP8 detrusor muscle. (B) Confocal image showing z-stacks of a 2 μm section of the trigone from a male SAMP8 bladder in which VAChT-ir nerves can be observed running parallel to the muscle bundles. (C) A high density of TH-ir adrenergic nerve trunks can be seen in the trigone from a male SAMR1 bladder. (D) Confocal image showing z-stacks of a 2 μm section of the trigone muscle layer from a female SAMR1 bladder in which abundant TH-ir nerves can be observed. Note the presence of TH-ir ganglion cells. Scale bar = 25 μm. Quantification of VAChT-ir (E) and TH-ir (F) in SAMR1 and SAMP8 bladders. Measurements were acquired independently in different regions of the bladder muscle layer (*dome, detrusor* and *trigone*). Hand-drawn fields of *whole-mount* preparations were selected and the area above the intensity threshold was measured (Area %). The values represent the mean ± SE of three to five different fields from four to six different animals: $^{*}P < 0.05$ versus SAMR1; $^{\#}P < 0.05$ versus female, and $^{\dagger}P < 0.05$, $^{\dagger\dagger}P < 0.01$ and $^{\dagger\dagger\dagger}P < 0.001$ versus the trigone region (ANOVA followed by Student's *t*-test).

Table 5

The pD_2 and E_{max} values obtained from the DEA/NO- and sildenafil-induced concentration-dependent relaxation curves in SAM-R1 and SAM-P8 urethras, and the effect of ODQ

	SAM-R1			SAM-P8		
	pD_2	E_{max} (% AVP)	*n*	pD_2	E_{max} (% AVP)	*n*
DEA/NO	4.90 ± 0.22	114 ± 14.7	12	5.22 ± 0.11	111 ± 15.4	9
DEA/NO + ODQ (0.1 mM)	3.63 ± 0.31$^{\#\#}$	124 ± 2.62	4	3.02 ± 0.13$^{\#\#\#}$	130 ± 4.60	4
Sildenafil	4.61 ± 0.11	113 ± 10.2	7	4.63 ± 0.10	98.5 ± 10.4	13
Sildenafil + ODQ (0.1 mM)	4.22 ± 0.13$^{\#\#}$	121 ± 12.8	4	4.1 ± 0.12$^{\#}$	109 ± 7.91	6

The E_{max} values (maximum response) are expressed as the percentage of the relaxation induced by 0.1 μM AVP. The pD_2 represents the negative logarithm of the agonist dose that induced 50% of the maximum response. The E_{max} and pD_2 are expressed as the mean ± SE: $^{\#}P < 0.05$, $^{\#\#}P < 0.01$, $^{\#\#\#}P < 0.001$ versus controls. No differences were found between SAMR1 and SAMP8 (ANOVA followed by Student's *t*-test).

Sustained urethral relaxation elicited by EFS (4 Hz, 4 min) or DEA/NO (0.1 mM, 4 min) was further studied in preparations that were pretreated with a cocktail of PDE inhibitors to directly compare relaxations and cGMP-ir (García-Pascual *et al.*, 2008). After an exposure of 30 s, PDE inhibitors produced relaxation in AVP pre-contracted preparations of 27 ± 4.4% in SAMR1 and 26 ± 3.7% in SAMP8 mice (n = 12 per group; Figure 10A and B). In preparations further exposed to DEA/NO (0.1 mM, 4 min; Figure 10A), relaxations peaked at 57 ± 5.6% in SAMR1 and 59 ± 3.1% in SAMP8 mice (n = 6 per group), while in those subjected to EFS (4 Hz, 4 min; Figure 10B) urethral relaxations of 45 ± 10.7% and 60 ± 5.1% were detected in SAMR1 and SAMP8 mice respectively (n = 6 per group). While the amplitude of relaxation was similar in

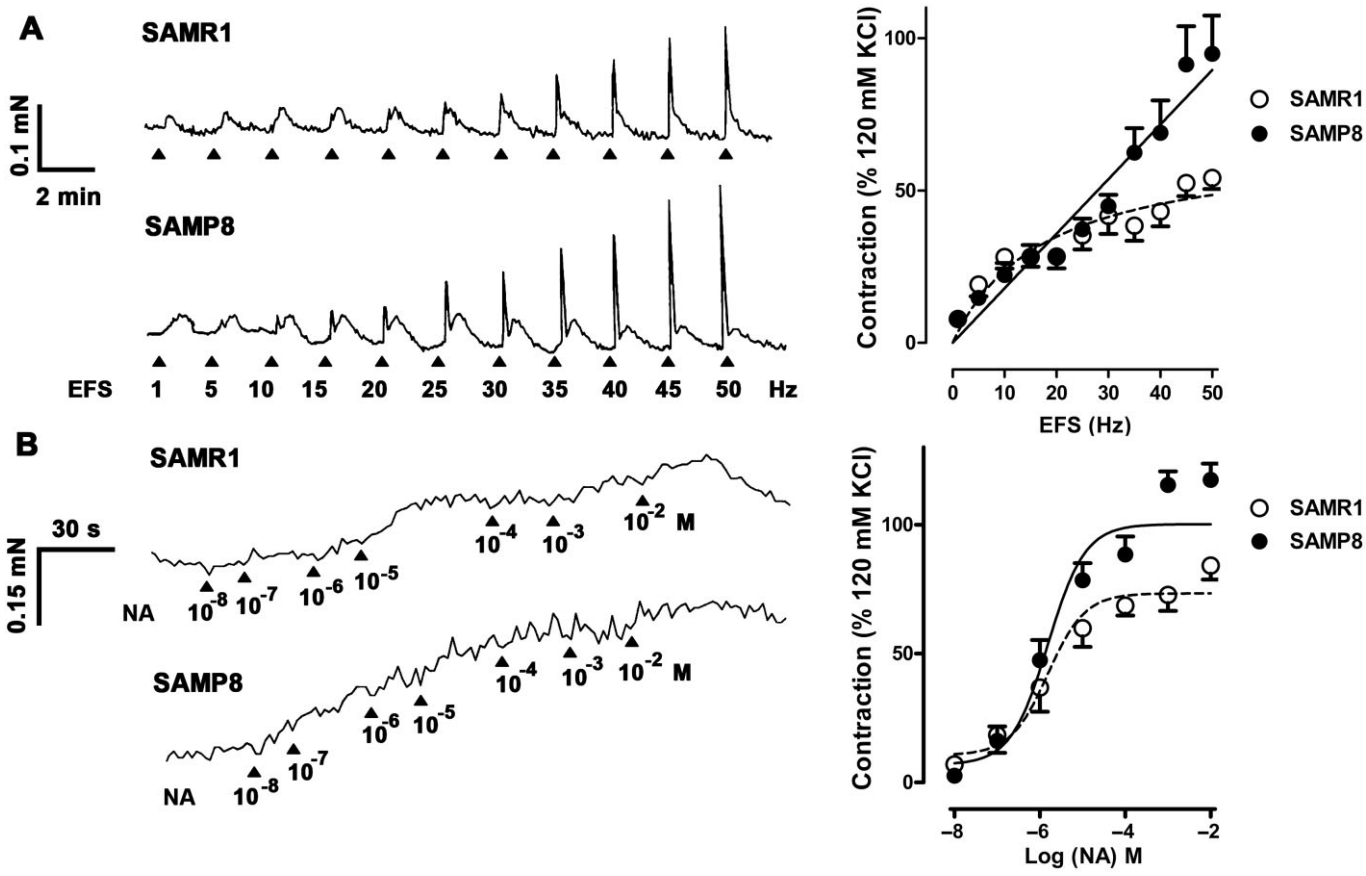

Figure 5

Contractile responses in SAMP8 and SAMR1 urethras. (*Left*) Representative traces showing SAMR1 (*top*) and SAMP8 (*bottom*) urethral contractions elicited by EFS (5 s, 1–50 Hz; A) and by cumulative addition of noradrenaline (10^{-8} to 10^{-2} M; B) in the presence of L-NOARG (0.1 mM) and D-tubocurarine (0.1 μM). (*Right*) Frequency–response curve (A) and concentration–response curve (B) for SAMR1 and SAMP8 urethras. The data are represented relative to the contraction induced by 120 mM KCl (mean ± SE; n = 10–13).

both strains, the slope, expressed as dF/dt (mN s^{-1}), revealed a faster relaxation in SAMP8 mice (Figure 10C). Pretreatment with L-NOARG and/or ODQ (both at 0.1 mM for 30 min) significantly reduced the dF/dt values for EFS- or DEA/NO-induced relaxations to a similar value in both strains (Figure 10A–C).

cGMP- and vimentin-ir in the urethra

Compared with basal conditions (in the presence of PDE inhibitors alone; Figure 11A and B), a 4 min exposure to DEA/NO produced (0.1 mM) a strong increase in cGMP-ir in both SAMR1 and SAMP8 urethras (Figure 11C and D), which was prevented by the presence of ODQ (0.1 mM, 30 min; Figure 11E and F). Quantification of cGMP-ir in DEA/NO-treated strips revealed a similar accumulation of cGMP in all regions of the urethra in both strains (Figure 11G). Moreover, the density of vimentin, a marker for ICs in the urethra (Garcia-Pascual *et al.*, 2008), was lower in the whole urethra of SAMP8 versus SAMR1 mice (Figure 12D). Confocal microscopy images showed that upon exposure to DEA/NO, cGMP- and vimentin-ir co-localized in a subset of spindle-shaped cells within the urethral muscle layer (Figure 12A–C). It should be noted that both markers were present in different subcellular domains, with strong vimentin-ir in the cytoplasmic prolongations and predominant cGMP-ir in the perinuclear cytosol (Figure 12C).

Discussion and conclusions

The observation of littermates of AKR/J mice that spontaneously became senile at an early age represented the starting point to generate the several lines of SAMP models currently available (Takeda *et al.*, 1981). The SAMP8 sub-strain has been used widely, mainly as a model for neurodegenerative disorders associated with ageing. However, the alterations to the gene expression and protein profiles in SAMP8 not only affect nerve-related proteins but also modify reactive oxygen metabolism (Butterfield and Poon, 2005) that is thought to be critical in cellular dysfunction associated with ageing.

In our study, SAMP8 mice (9–10 months of age) exhibited both external and behavioural signs of ageing similar to those reported previously (Takeda *et al.*, 1981; 1997). The LUT of SAMP8 mice revealed no apparent tumourigenic processes or

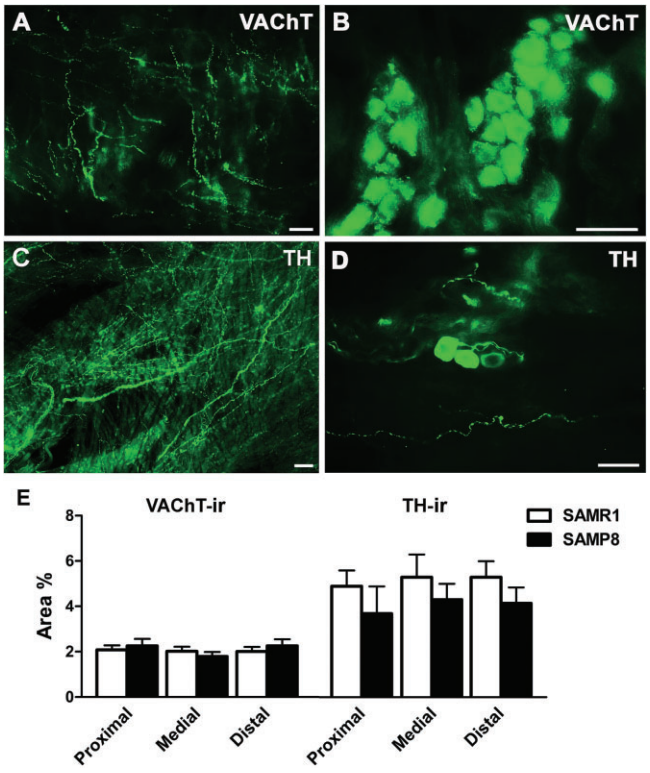

Figure 6

VAChT- and TH-ir in SAMR1 and SAMP8 urethras. Cholinergic VAChT-ir nerves (A) and intramural ganglion cells (B) in the proximal region of the SAMP8 urethral muscle layer. (C) Abundant TH-ir adrenergic innervation in the proximal region of the urethra in a SAMR1 mouse. (D) TH-ir intramural ganglion cells in the distal region of the urethra in a SAMP8 mouse. Scale bar = 25 μm. (E) Quantification of VAChT-ir and TH-ir in SAMR1 and SAMP8 urethras. Measurements were taken independently in different regions of the urethral muscular layer (*proximal, medial* and *distal*). Hand-drawn fields of *whole-mount* preparations were selected and the area above the intensity threshold was measured (Area %). The values represent the mean ± SE of four to five different fields from four to five different animals.

other pathological events, although inflammatory cells were occasionally observed being consistent with the increased inflammatory activity associated with ageing (Phillips and Davies, 1980). The LUT of SAMP8 mice had a comparable relative weight to that of their SAMR1 counterparts and their histological appearance seemed to exclude structural changes. Furthermore, the contractions induced by high concentrations of K^+ in the SAMP8 and SAMR1 bladder and urethra of the same sex suggest that ageing did not significantly impair the basic mechanisms underlying smooth muscle contraction, such as Ca^{2+} entry via voltage-operated calcium channels and actin–myosin or Ca^{2+}–calmodulin interactions (Saito *et al.*, 1993; Lluel *et al.*, 2000; Yoshida *et al.*, 2001). Accordingly, the changes in contractility reported here were probably of neurogenic origin and due to alterations in the release and/or postsynaptic action of transmitters. In both strains, the bladder of males is larger and male bladder preparations produced greater contractions than that of females, as in other species and in humans (Pessina *et al.*, 2007; Schneider *et al.*, 2011). Males also showed a higher micturition frequency, possibly related to their territorial behaviours. Despite these sexual differences, the study clearly showed an increase in micturition frequency in aged animals of both sexes, suggesting the appearance of some form of bladder overactivity with ageing.

The neurogenic detrusor contraction in SAMR1 mice had a prominent cholinergic origin, as reported in other species (Andersson and Wein, 2004), as well as a purinergic component that was proportionally more important in the females. EFS-induced detrusor contractions were stronger in senescent animals of both sexes with a similar relative participation of the cholinergic and purinergic components. This would imply a stronger increase in the purinergic contribution to male bladder activity with ageing, while no such changes in the relative involvement of these two components were observed in females. No changes in cholinergic innervation were evident in either gender, although the sensitivity to exogenously added ACh was heightened in male but not in female SAMP8 mice. This sensitization could be due to an increase in the number of receptors (Kolta *et al.*, 1984) or to a shift in receptor subtype (Ruggieri and Braverman, 2006; Michel and Barendrecht, 2008).

Reported changes in ACh- or charbachol-induced bladder contractions of aged rats and humans are contradictory (see Michel and Barendrecht, 2008). In most studies, reductions (Zhao *et al.*, 2010) or no change (Lluel *et al.*, 2000; Kosan *et al.*, 2008) in cholinergic contractions are described, although our results in female SAMP8 mice are consistent with previous findings in female C57 mice (Lagou *et al.*, 2006). It cannot be ruled out that increased ACh release driven by presynaptic adrenergic (Yamamoto *et al.*, 2001) and/or cholinergic receptors (Braverman *et al.*, 1998) could participate in the enhanced responses to EFS. Indeed, presynaptic muscarinic facilitation may underlie the increased bladder contractility in rats with spinal injury (Somogyi *et al.*, 1998). Non-neuronal ACh release has also been described in elderly patients (Yoshida *et al.*, 2004), probably of urothelial origin (Pinna *et al.*, 1996; Fry *et al.*, 2010), and this is a possibility that we cannot disregard given the strong urothelial VAChT-ir observed (data not shown).

The parallel augmentation of the purinergic component, more evident in the aged male detrusor, could be due to the increased sensitivity to ATP, as reported in aged humans, rats and other mouse strains (Kageyama *et al.*, 2000; Wuest *et al.*, 2005; Lai *et al.*, 2007), and it is consistent with the increase in the atropine-resistant component of bladder contraction in several bladder pathologies (Fry *et al.*, 2010). Changes in ecto-ATPase activity (Harvey *et al.*, 2002), or in the expression of purinergic receptors (Suadicani *et al.*, 2009), could increase ATP levels in ageing. However, our results suggest the appearance of a third component in SAMP8 female bladder contractions: a prostanoid that accounts for 15–20% of the detrusor contraction. COX inhibitors influence bladder hyperactivity (Roosen *et al.*, 2009) and rats treated with EP_1 receptor antagonists display increased bladder capacity (Lee *et al.*, 2007). Furthermore, increased levels of urinary PGE_2 and $PGF_{2\alpha}$ have been reported in women with overactive bladders (Kim *et al.*, 2006; McCafferty *et al.*, 2008), and higher levels of 8-epi-$PGF_{2\alpha}$ have been associated with ageing in rabbits

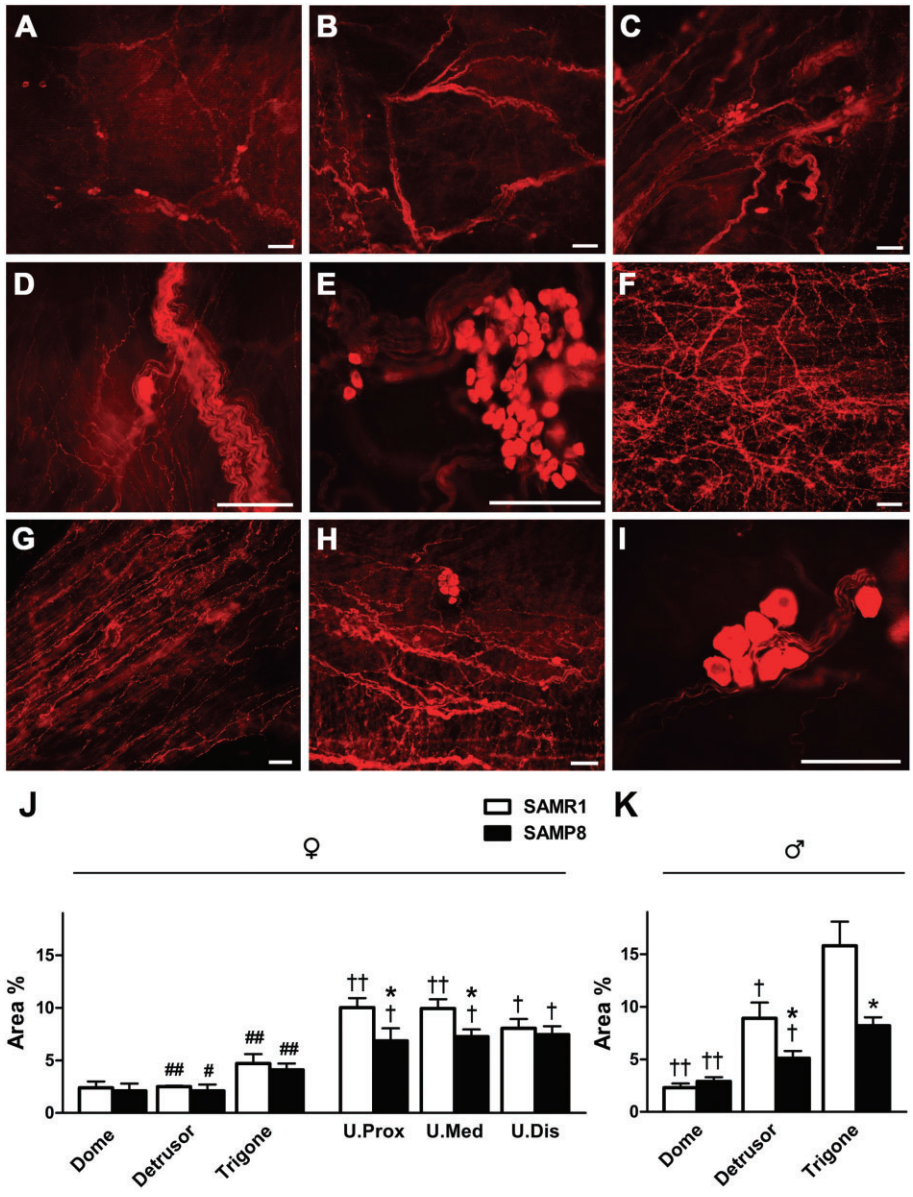

Figure 7

nNOS-ir in SAMR1 and SAMP8 bladders and urethras. (A) nNOS-ir in the bladder dome from a female SAMR1 mouse showing the dispersion of the nitrergic nerves. Note the scattered presence of small nNOS-ir ganglion cells. nNOS-ir in the detrusor (B) and trigone (C) from a male SAMP8 mouse. An increased density of nitrergic nerves, ganglia and nerve trunks is apparent in the trigone. Higher magnification image showing nNOS-positive nerve trunks and intramural ganglion cells positive for nNOS in the trigone of a female (D) and a male (E) SAMR1 mouse. (F) nNOS-ir in the medial urethra of a SAMR1 mouse showing abundant nitrergic innervation. nNOS-ir in the proximal (G) and distal (H) SAMP8 urethra: note the slight reduction in nitrergic nerve density compared with the SAMR1 urethra (F). (I) High magnification image showing nNOS-positive intramural ganglion cells in the medial urethra of a SAMP8 mouse. Scale bar = 50 μm. Quantification of nNOS-ir in the muscle layer of SAMR1 and SAMP8 female bladders and urethras (J), and in male bladders (K). Measurements were taken independently in different regions of the bladder (*dome*, *detrusor* and *trigone*) and urethral muscle layers (*proximal*, *medial* and *distal*). Hand-drawn fields of *whole-mount* preparations were selected and the relative area above the intensity threshold was measured (Area %). The values represent the mean ± SE of four to five different fields from five to seven different animals: $^{*}P < 0.05$ versus SAMR1; $^{\#}P < 0.05$ and $^{\#\#}P < 0.01$ versus male; $^{\dagger}P < 0.05$ and $^{\dagger\dagger}P < 0.01$ versus the trigone region (ANOVA followed by Student's *t*-test).

(Tarcan *et al.*, 2000). Finally, only male SAMP8 mice exhibited a significant reduction in TH-ir nerves similar to that described in aged rats (Warburton and Santer, 1994). Reduced noradrenaline release might diminish bladder filling during the continence phase due to a reduction in presynaptic inhibition through the α_1-adrenoceptors on parasympathetic nerves, and through its direct relaxant influence via β-adrenoceptor activation (Andersson and Arner, 2004).

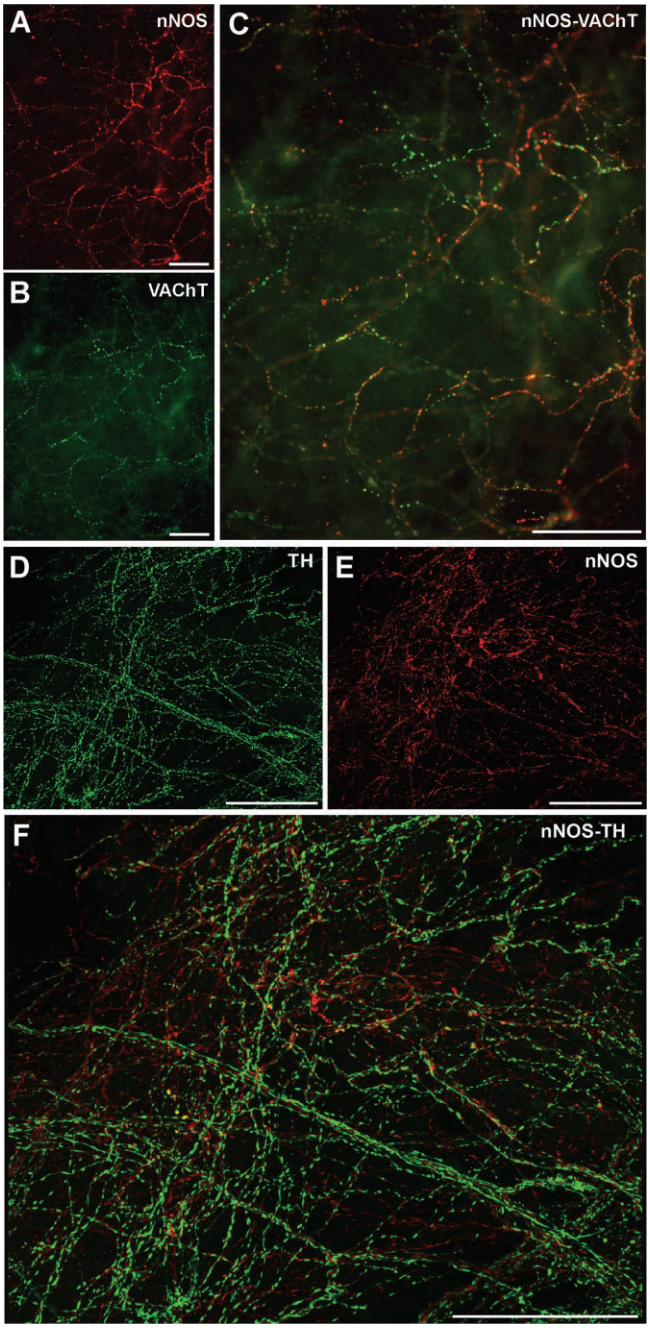

Figure 8

Dual labelling of nNOS-ir/VAChT-ir and nNOS-ir/TH-ir in the urethral muscular layer. Representative photomicrographs of nNOS-ir (A, E), VAChT-ir (B) and TH-ir (D), along with the corresponding merged images (C, F). (A–C) Fluorescence images from a SAMP8 proximal urethra showing the co-localization of nNOS and VAChT in a dense nerve network. (D–F) Confocal images showing z-stacks of a 2 µm section of a SAMR1 proximal urethra showing similar patterns of nNOS- and TH-ir in varicosities of thin fibre networks that were completely segregated yet closely related. Scale bar = 50 µm.

Moreover, the marked decrease in bladder neck TH-ir could lead to incomplete closure of the muscle sphincter during continence.

In the mouse urethra, for the first time we describe a biphasic contraction in response to EFS, similar to that reported in the rabbit and human urethra (Mattiasson *et al.*, 1985; Deplanne *et al.*, 1998), a response mediated by phentolamine-sensitive α-adrenoceptors, comparable to that reported in other species (Garcia-Pascual *et al.*, 1991; Andersson, 1993). The dense TH-ir nerve network seen here provides a morphological correlate for noradrenaline release. EFS-induced contractions increased at high frequencies in aged SAMP8 mice in contrast to that reported in rats (Lluel *et al.*, 2003), this was predominantly associated with the fast component. Furthermore, the urethral sensitization to noradrenaline might underlie such increase because no changes in TH-ir were detected. Similarly, age-associated adrenergic hypersensitivity has been described in the rabbit and dog urethra, probably related to an increase in the number of α-adrenoceptors (Yoshida *et al.*, 1991; Suzuki *et al.*, 1999).

NO released from nitrergic nerves seems to be the main element responsible for the urethral relaxation induced by EFS (Andersson *et al.*, 1992; Persson *et al.*, 2000). Indeed, EFS-induced nitrergic relaxations were inhibited by L-NOARG in both strains and a dense network of nNOS-ir nerves is present in the urethral muscle which increased from the bladder to the outlet region in both sexes of either strain, as found in other species and humans (Persson *et al.*, 1993; Triguero *et al.*, 1993; Leone *et al.*, 1994). Such a distribution is consistent with the leading role of urethral nitrergic relaxation in the onset of micturition. For this reason, the rest of the experiments focused on the female urethra.

SAMP8 mice had a lower density of nNOS-ir and weaker urethral EFS-induced nitrergic relaxation than SAMR1 ones. A similar attenuation of nitrergic relaxation has been described in urinary dysfunction associated with diabetes (Mumtaz *et al.*, 1999) and in the intestinal smooth muscle of aged animals (Takeuchi *et al.*, 1998), which showed decreased levels of NO (Mármol *et al.*, 2009). Furthermore, the decrease in nNOS-ir in SAMP8 mice might attenuate the presynaptic inhibition of adrenergic nerves by NO (Andersson and Wein, 2004), provoking increased noradrenaline release and then enhanced contractility. In fact, confocal microscopy revealed closed appositions between segregated TH-ir and nNOS-ir networks that could permit presynaptic modulation of noradrenaline release by NO from neighbouring nerves.

Dysfunction of the NO/cGMP pathway has been implicated in bladder hyperactivity, which can be ameliorated by increasing cGMP levels and through specific PDE5 inhibitors, such as sildenafil (Morelli *et al.*, 2009). The effect of ODQ confirms that the urethral relaxation induced by sildenafil or DEA/NO was GC dependent. However, we found no differences in the relaxation induced by either drug, thus suggesting that GC activation is not altered in aged animals. Indeed, the urethral cGMP-ir in response to DEA/NO was similar in both strains. However, kinetic analysis revealed a marked increase in the rate of nitrergic relaxation in SAMP8 mice. This sensitization appears to involve the NO/cGMP pathway as it was attenuated by the inhibition of GC (ODQ) or NOS (L-NOARG). Moreover, it may be directly triggered by NO as

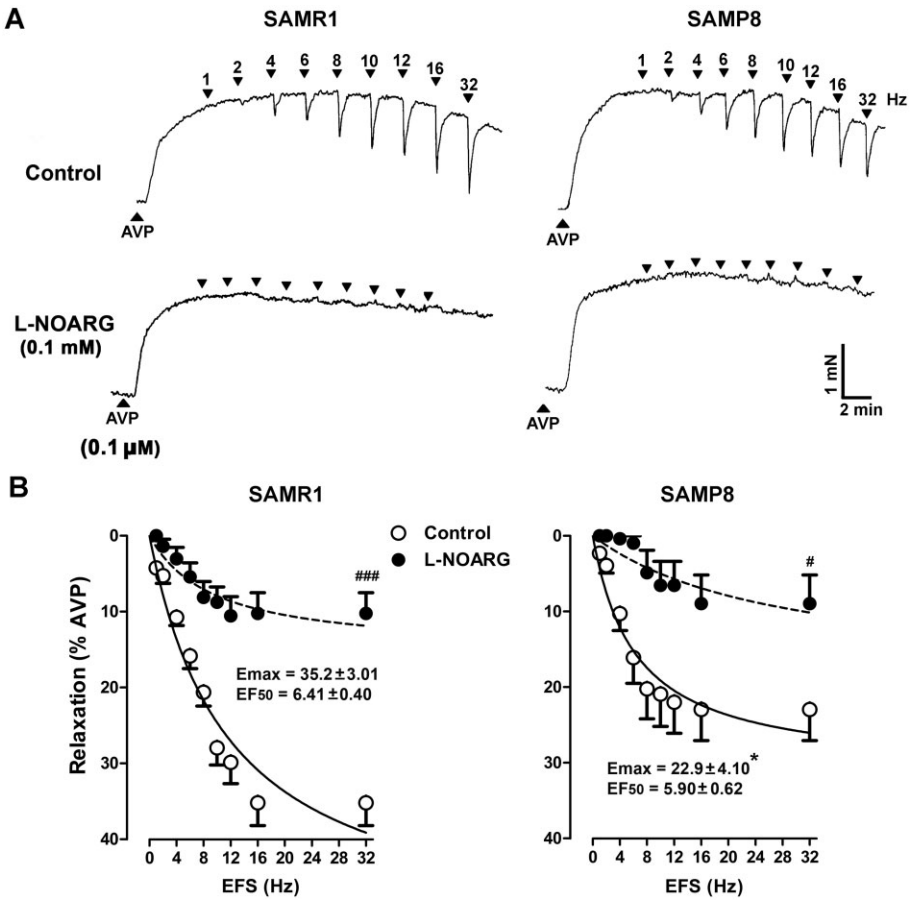

Figure 9

Frequency-dependent relaxant responses in female SAMR1 and SAMP8 urethras. (A) Representative traces showing SAMR1 (*left*) and SAMP8 (*right*) urethral relaxations elicited by EFS (5 s, 1–32 Hz) in AVP (0.1 µM) pre-contracted urethral preparations maintained in the presence of atropine (1 µM) and guanethidine (50 µM). The effect of a 30 min pretreatment with L-NOARG (0.1 mM, *bottom*) is also shown. (B) Frequency–response relaxation curves in SAMR1 (*left*) and SAMP8 (*right*) urethral preparations under control conditions (open symbols) and after a 30 min pretreatment with L-NOARG (0.1 mM; filled symbols). The data represent the mean ± SE (n = 6–14) and they are expressed relative to the contraction induced by AVP (0.1 µM). The E_{max} and EF_{50} values from the respective control curves (SAMR1; n = 16 and SAMP8; n = 14) are included in the figure: $^{*}P < 0.05$ SAMP8 versus SAMR1; $^{\#}P < 0.05$; $^{\#\#\#}P < 0.001$ L-NOARG-treated preparations versus controls.

it was elicited by either DEA/NO or EFS-stimulated neuronal NO release. Sensitization to NO could be viewed as a compensatory response to the loss of nitrergic innervation in aged animals, although the underlying mechanism remains to be established.

DEA/NO-induced accumulation of cGMP in the urethra was mainly observed in vimentin-positive ICs, in line with results from the sheep and rat urethra where ICs were proposed as intermediates in urethral nitrergic neurotransmission due to the tight anatomical relationship between ICs and nNOS-ir nerves, the selective stimulation of intramuscular ICs upon nitrergic EFS and the probable involvement of cGMP-gated cationic channels expressed in ICs in such neurotransmission (Garcia-Pascual *et al.*, 2008; Triguero *et al.*, 2009). The results presented here support this description of the mouse urethra, and, moreover, the concomitant reduction in nNOS-ir nerves and vimentin-ir ICs in the SAMP8 urethra suggests a close functional relationship between nitrergic nerves and ICs. Indeed, a trophic effect of nitrergic nerves on ICs has been described in the guinea pig bladder (de Jongh *et al.*, 2007). Urethral ICs have been attributed a prominent role as pacemakers of the myogenic tone of the urethra (Sergeant *et al.*, 2000), and thus their loss with ageing could lower urethral closure pressure and negatively affect continence. Similar IC reductions with age have been described in the gastrointestinal tract (Gómez-Pinilla *et al.*, 2011). It should be noted that we did not find differences in the density of cGMP-ir following exposure to DEA/NO in the intramuscular IC population. It has been suggested that there may be distinct functional subpopulations of vimentin-ir urethral ICs, only one of which accumulates cGMP upon nitrergic stimulation (Garcia-Pascual *et al.*, 2008). Our results could be explained by the differential effects of ageing on the distinct populations of ICs, whereby those participating in nitrergic relaxation might be more resistant, possibly reflecting a compensatory response to the overall reduction in urethral nitrergic innervation in aged animals.

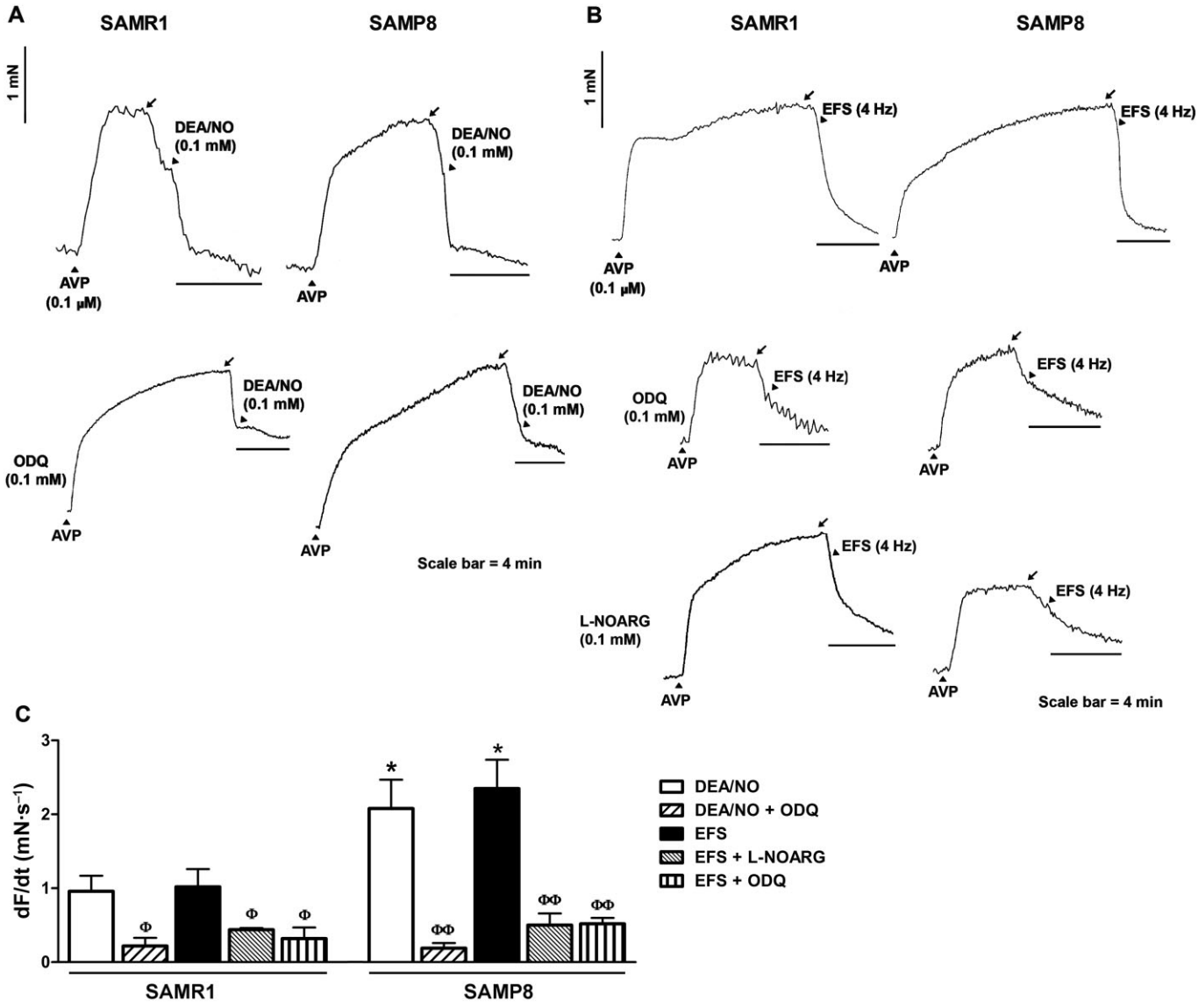

Figure 10

Long-duration relaxation responses induced by DEA/NO or EFS in female SAMR1 and SAMP8 urethras. (A and B) Representative traces showing relaxant responses induced by stimulation with (A) DEA/NO (0.1 mM) or (B) EFS (4 Hz) for 4 min in AVP (0.1 μM) pre-contracted urethral preparations from SAMR1 (*left*) and SAMP8 (*right*) mice in the presence or absence of the PDE inhibitors IBMX and zaprinast (0.1 mM, each administered 30 s before stimulation). Lower panels show the effects of ODQ and L-NOARG (both at 0.1 mM). The black arrows indicate the point at which the PDE inhibitors were added. (C) Slope of the relaxation responses induced by DEA/NO (0.1 mM) and EFS (4 Hz) treatment for 4 min in AVP (0.1 μM) pre-contracted urethral preparations from SAMR1 and SAMP8 mice in the presence of IBMX (1 mM) and zaprinast (0.1 mM) administered 30 s before stimulation, and in the presence or absence of L-NOARG or ODQ (0.1 mM each). The data represent the mean ± SE (n = 4–6): *$P < 0.05$ versus SAM-R1; $^{\Phi}P < 0.05$, $^{\Phi\Phi}P < 0.01$ versus control preparations (ANOVA followed by Student's t-test).

In conclusion, we have observed a significant increase in the micturition frequency of aged mice, which was accompanied by increased bladder and urethral contractile responses provoked by excitatory influences. Furthermore, our findings reveal a concomitant impairment of urethral relaxation in aged female animals, which may be linked to the reduction in the nitrergic innervation and/or in IC density, but not by mechanisms involving cGMP. Our results suggest that the SAMP8 mouse model is a useful experimental tool to study LUT disorders during ageing and to use in the search for new therapeutic targets.

Acknowledgements

This work was supported by grants from the 'Comunidad de Madrid – Universidad Complutense de Madrid' (UCMGR85/06-920307), the UCM-Santander (GR35/10-A-920307) and

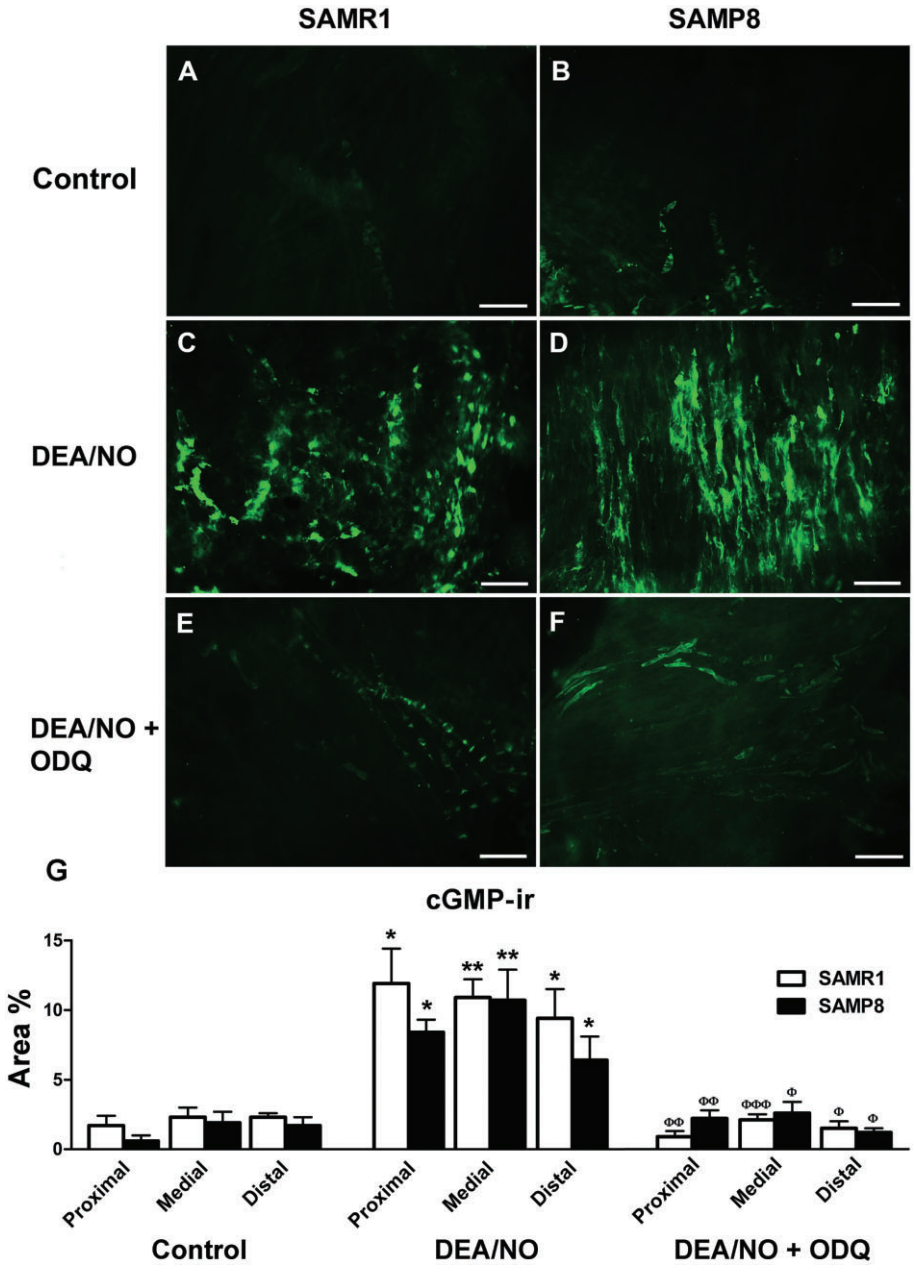

Figure 11

cGMP-ir in SAMR1 and SAMP8 urethras. (A–F) Representative microphotographs showing cGMP-ir in the medial urethra of SAMR1 (A, C, E) and SAMP8 (B, D, F) mice in the presence of IBMX and zaprinast alone (1 and 0.1 mM, respectively, for 4 min; A, B, *controls*), as well as after the addition of DEA/NO (0.1 mM, 4 min)\ in the presence (E, F) or absence (C, D) of ODQ (0.1 mM). The experimental protocol used is described in Figure 10. Note the weak cGMP-ir in control conditions (A, B) compared with that induced by DEA/NO (C, D), and the dramatic reduction in cGMP-ir following exposure to ODQ (E, F). Scale bar = 50 μm. (G) Quantification of cGMP-ir in the SAMR1 and SAMP8 urethras. Measurements were taken independently in different regions of the urethral muscular layer (*proximal*, *medial* and *distal*). Hand-drawn fields of *whole-mount* preparations were selected and the relative area above the intensity threshold was measured (Area %). The values represent the mean ± SE of three to five different fields from four to five different animals: $^{*}P < 0.05$ and $^{**}P < 0.01$ versus controls; $^{\Phi}P < 0.05$, $^{\Phi\Phi}P < 0.01$ and $^{\Phi\Phi\Phi}P < 0.001$ versus preparations exposed to DEA/NO in the absence of ODQ (ANOVA followed by Student's *t*-test).

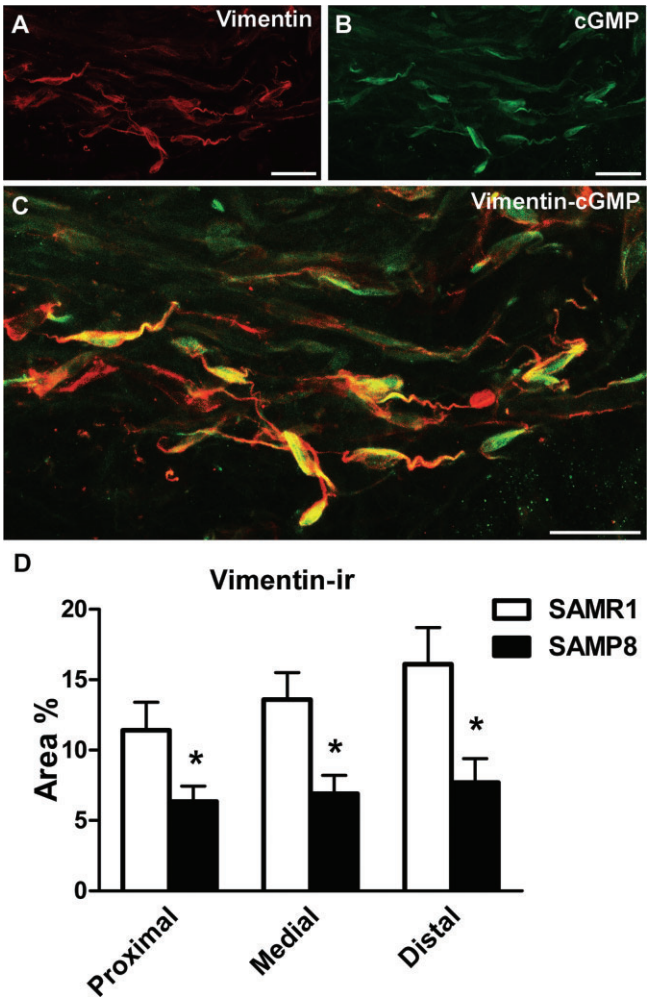

Figure 12

Vimentin-ir in SAMR1 and SAMP8 urethras and its co-localization with cGMP-ir. (A–C) Representative confocal images showing z-stacks of a 2 μm section from the proximal SAMR1 urethra treated with DEA/NO (0.1 mM, 4 min). Vimentin-ir (A, red) and cGMP-ir (B, green) are shown along with the corresponding merged image (C). Note the co-localization of vimentin-ir and cGMP-ir in numerous spindle-shaped ICs, in which vimentin-ir is mainly concentrated at the periphery of the cell and in the cell processes in particular, while cGMP-ir predominantly accumulates in the cytosol. Scale bar = 10 μm. (D) Quantification of vimentin-ir in SAMR1 and SAMP8 urethras. Measurements were taken independently in different regions of the urethral muscular layer (*proximal*, *medial* and *distal*). Hand-drawn fields of *whole-mount* preparations were selected and the relative area above the intensity threshold was measured (Area %). The values represent the mean ± SE of three to five different fields from four to six different animals: $*P < 0.05$ versus SAMR1 (ANOVA followed by Student's *t*-test).

the Fundación Mutua Madrileña (FMM2011). The micro-photographs presented were acquired and analysed at the Microscopy and Cytometry Centre (Complutense University, Madrid, Spain) with the technical assistance of Alfonso Cortés and Luis M. Alonso.

Conflict of interest

None.

References

Alexander SPH, Benson HE, Faccenda E, Pawson AJ, Sharman JL Spedding M *et al.* (2013a), The Concise Guide to PHARMACOLOGY 2013/14: Enzymes. Br J Pharmacol, 170: 1797–1867

Alexander SPH, Benson HE, Faccenda E, Pawson AJ, Sharman JL, Catterall WA *et al.* (2013b), The Concise Guide to PHARMACOLOGY 2013/14: Ligand-Gated Ion Channels. Br J Pharmacol 170: 1582–1606.

Alexander SPH, Benson HE, Faccenda E, Pawson AJ, Sharman JL Spedding M *et al.* (2013c), The Concise Guide to PHARMACOLOGY 2013/14: G Protein-Coupled Receptors. Br J Pharmacol 170: 1459–1581.

Andersson KE (1993). Pharmacology of the lower urinary tract smooth muscles and penile erectile tissues. Pharmacol Rev 45: 253–308.

Andersson KE, Arner A (2004). Urinary bladder contraction and relaxation: physiology and pathophysiology. Physiol Rev 84: 935–986.

Andersson KE, Wein AJ (2004). Pharmacology of the lower urinary tract: basis for current and future treatments of urinary incontinence. Pharmacol Rev 56: 581–631.

Andersson KE, Garcia-Pascual A, Persson A, Forman A, Tøttrupt A (1992). Electrically-induced nerve-mediated relaxation of rabbit urethra involves nitric oxide. J Urol 147: 253–259.

Braverman AS, Kohn IJ, Luthin GR, Ruggieri MR (1998). Prejunctional M_1 facilitatory and M_2 inhibitory muscarinic receptors mediate rat bladder contractility. Am J Physiol 274: R5177–RR523.

Butterfield DA, Poon HF (2005). The senescence-accelerated prone mouse (SAMP8): a model of age-related cognitive decline relevance to alterations of the gene expression and protein abnormalities in Alzheimer's disease. Exp Gerontol 40: 774–783.

Coyne KS, Sexton CC, Thompson CL, Milson I, Irwin D, Kopp ZS *et al.* (2009). The prevalence of lower urinary tract symptoms (LUTS) in the USA, UK and Sweden: results from the Epidemiology of LUTS (EpiLUTS) study. BJU Int 104: 352–360.

Deplanne V, Palea S, Angel I (1998). The adrenergic, cholinergic and NANC nerve-mediated contractions of the female rabbit bladder neck and proximal, medial and distal urethra. Br J Pharmacol 123: 1517–1524.

Dickson A, Avelino A, Cruz F, Ribeiro-da-Silva A (2006). Peptidergic sensory and parasympathetic fiber sprouting in the mucosa of the rat urinary bladder in a chronic model of cyclophosphamide-induced cistitis. Neuroscience 141: 1633–1647.

Forman K, Vara E, Garcia C, Kireev R, Cuesta S, Escames G *et al.* (2011). Effect of a combined treatment with growth hormone and melatonin in the cardiological ageing on male SAMP8 mice. J Gerontol A Biol Sci Med Sci 66: 823–834.

Fry CH, Meng E, Young JS (2010). The physiological function of lower urinary tract smooth muscle. Auton Neurosci 154: 3–13.

Garcia-Pascual A, Costa G, Garcia-Sacristán A, Andersson KE (1991). Calcium-dependence of contractile activation of isolated sheep urethra. I: responses to electrical stimulation. Pharmacol Toxicol 69: 263–269.

Garcia-Pascual A, Sancho M, Costa G, Triguero D (2008). Interstitial cells of Cajal in the urethra are cyclic GMP-mediated targets of nitrergic neurotransmission. Am J Physiol Renal Physiol 295: F971–F983.

Gómez-Pinilla PJ, Gibbons SJ, Sarr MG, Kendrick ML, Shen R, Cima RR *et al*. (2011). Changes in interstitial cells of Cajal with age in the human stomach and colon. Neurogastroenterol Motil 23: 36–44.

Harvey RA, Skennerton DE, Newgreen D, Fry CH (2002). The contractile potency of adenosine triphosphate and ecto-adenosine triphosphatase activity in guinea pig detrusor and detrusor from patients with a stable, unstable or obstructed bladder. J Urol 168: 1235–1239.

Irwin DE, Milson I, Hunskaar S, Reilly K, Kopp Z, Herschorn S *et al*. (2006). Population-based survey of urinary incontinence, overactive bladder and other lower urinary tract symptoms in five countries: results of the EPIC study. Eur Urol 50: 1306–1314.

de Jongh R, van Koeveringe GA, van Kerrebroeck PE, Markerink-van Ittersum M, de Vente J, Gillespie JI (2007). Alterations to network of NO/cGMP-responsive interstitial cells induced by outlet obstruction in guinea-pig bladder. Cell Tissue Res 330: 147–160.

Kageyama S, Fujita K, Suzuki K, Shinbo H, Masuda N, Uchida W (2000). Effect of age on the responses of rat bladder detrusor strips to adenosine triphosphate. BJU Int 85: 899–904.

Kilkenny C, Browne W, Cuthill IC, Emerson M, Altman DG (2010). Animal research: reporting *in vivo* experiments: the ARRIVE guidelines. Br J Pharmacol 160: 1577–1579.

Kim JC, Park EY, Seo SI, Park YH, Hwang TK (2006). Nerve growth factor and prostaglandins in urine from female patients with overactive bladder. J Urol 175: 1773–1776.

Kolta MG, Wallace LJ, Gerald MC (1984). Age-related changes in sensitivity of rat urinary bladder to autonomic agents. Mech Ageing Dev 27: 183–188.

Kosan M, Tul M, Ozturk B, Hafez G, Inal G, Cetinkaya M (2008). Alteration in contractile responses in human detrusor smooth muscle from obstructed bladders with overactivity. Urol Int 80: 193–200.

Lagou M, Gillespie J, Kirkwood T, Harvey I, Drake MJ (2006). Muscarinic stimulation of the mouse isolated whole bladder: physiological responses in young and ageing mice. Auton Autacoid Pharmacol 26: 253–260.

Lai HH, Boone TB, Thompson TC, Smith CP, Somogyi GT (2007). Using caveolin-1 knockout mouse to study impaired detrusor contractility and disrupted muscarinic activity in the ageing bladder. Urology 69: 407–411.

Lee T, Hedlund P, Newgreen D, Andersson KE (2007). Urodynamic effects of a novel EP1 receptor antagonist in normal rats and rats with bladder outlet obstruction. J Urol 177: 1562–1567.

Leone AM, Wilklund NP, Hökfelt T, Brundin L, Moncada S (1994). Release of nitric oxide by nerve stimulation in the human urogenital tract. Neuroreport 5: 733–736.

Lluel P, Palea S, Barras M, Grandadam F, Heudes D, Bruneval P *et al*. (2000). Functional and morphological modifications of the urinary bladder in aging female rats. Am J Physiol 278: R964–R972.

Lluel P, Deplanne V, Hendes D, Bruneval P, Polea S (2003). Age-related changes in urethrovesical coordination in male rats: relationship with bladder instability? Am J Physiol 284: R1287–R1295.

McCafferty GP, Misajet BA, Laping NJ, Edwards RM, Thorneloe KS (2008). Enhanced bladder capacity and reduced prostaglandin E2-mediated bladder hyperactivity in EP3 receptor knockout mice. Am J Physiol Renal Physiol 295: F507–F514.

McGrath J, Drummond G, McLachlan E, Kilkenny C, Wainwright C (2010). Guidelines for reporting experiments involving animals: the ARRIVE guidelines. Br J Pharmacol 160: 1573–1576.

Mármol F, Sánchez J, López D, Martínez N, Mitjavila MT, Puig-Parellada P (2009). Oxidative stress, nitric oxide and prostaglandins E2 levels in the gastrointestinal tract of aging rats. J Pharm Pharmacol 61: 201–206.

Mattiasson A, Andersson KE, Sjögren C (1985). Adrenergic and non-adrenergic contraction of isolated urethral muscle from rabbit and man. J Urol 133: 298–303.

Michel MC, Barendrecht MM (2008). Physiological and pathological regulation of the autonomic control of urinary bladder contractility. Pharmacol Ther 117: 297–312.

Morelli A, Filippi S, Sandner P, Fibbi B, Chavalmane AK, Silvestrini E *et al*. (2009). Vardenafil modulates bladder contractility through cGMP-mediated inhibition of RhoA/Rho kinase signaling pathway in spontaneously hypertensive rats. J Sex Med 6: 1594–1608.

Mumtaz FH, Sullivan ME, Thompson CS, Dashwood MR, Naseem KM, Bruckdorfer KR *et al*. (1999). Alterations in the nitric oxide synthase binding sites and non-adrenergic, non-cholinergic mediated smooth muscle relaxation in the diabetic rabbit bladder outlet: possible relevance to the pathogenesis of diabetic cystopathy. J Urol 162: 558–566.

Persson K, Alm P, Johansson K, Larsson B, Andersson KE (1993). Nitric oxide synthase in pig lower urinary tract: immunohistochemistry, NADPH diaphorase histochemistry and functional effects. Br J Pharmacol 110: 521–530.

Persson K, Pandita RK, Aszòdi A, Ahmad M, Pfeifer A, Fässler R *et al*. (2000). Functional characteristics of urinary tract smooth muscles in mice lacking cGMP protein kinase type I. Am J Physiol Regul Integr Comp Physiol 279: R1112–R1120.

Pessina F, Valeri A, Dragoni S, Valoti M, Sgaragli G (2007). Gender-related neuronal and smooth muscle damage of guinea pig isolated urinary bladder from anoxia-glucopenia and reperfusion injury and its relationship to glycogen content. Neurourol Urodyn 26: 416–423.

Phillips JL, Davies I (1980). The comparative morphology of the bladder and urethra in young and old female C57BL/Icrfa mice. Exp Gerontol 15: 551–562.

Pinna C, Ventura F, Puglisi L, Burnstock G (1996). A pharmacological and histochemical study of hamster urethra and the role of urothelium. Br J Pharmacol 119: 655–662.

Roosen A, Chapple CR, Dinochowski RR, Fowler CJ, Gratze C, Roehrborn CG *et al*. (2009). A refocus on the bladder as the originator of storage lower urinary tract symptoms: a systematic review of the latest literature. Eur Urol 56: 810–820.

Ruggieri MR, Braverman AS (2006). Regulation of bladder muscarinic receptor subtypes by experimental pathologies. Auton Autacoid Pharmacol 26: 311–325.

Saito M, Kondo A, Gotoh M, Kato K, Levin M (1993). Age-related changes in the response of the rat urinary bladder to neurotransmitters. Neurourol Urodyn 12: 191–200.

Schneider T, Fetscher C, Michel MC (2011). Human urinary bladder strip relaxation by the β-adrenoceptor agonist isoprenaline: methodological considerations and effects of gender and age. Front Pharmacol 2: 11.

Sergeant GP, Hollywood MA, McCloskey KD, Thornbury KD, McHale NG (2000). Specialised pacemaking cells in the rabbit urethra. J Physiol 526: 359–366.

Somogyi GT, Zernova GV, Yoshiyama M, Yamamoto T, de Groat WC (1998). Frequency dependence of muscarinic facilitation of transmitter release in urinary bladder strips from neutrally intact or chronic spinal cord transected rats. Br J Pharmacol 125: 241–246.

Suadicani SO, Urban-Maldonado M, Tar MT, Melman A, Spray DC (2009). Effects of ageing and streptozotocin-induced diabetes on connexin43 and P2 purinoceptor expression in the rat corpora cavernosa and urinary bladder. BJU Int 103: 1686–1693.

Suzuki M, Moriyama N, Okaya Y, Nishimatsu H, Kawabe K, Aisaka K (1999). Age-related change of the role of α_{1L}-adrenoceptor in canine urethral smooth muscle. Gen Pharmacol 33: 347–354.

Takeda T, Hosokawa M, Takeshita S, Irino M, Higuchi K, Matsushita T *et al*. (1981). A new murine model of accelerated senescence. Mech Ageing Dev 17: 183–194.

Takeda T, Matsushita T, Kurozumi M, Takemura K, Higuchi K, Hosokawa M (1997). Pathobiology of the senescence-accelerated mouse (SAM). Exp Gerontol 32: 117–127.

Takeuchi T, Niioka S, Yamaji M, Okishio Y, Ishii T, Nishio H *et al*. (1998). Decrease in participation of nitric oxide in non-adrenergic non-cholinergic relaxation of rat intestine with age. Jpn J Pharmacol 78: 293–302.

Tarcan T, Siroky MB, Krane RJ, Azadzoi KM (2000). Isprostane 8-epi PGF2α, a product of oxidative stress, is synthesized in the bladder and causes detrusor smooth muscle contraction. Neurourol Urodyn 19: 43–51.

Triguero D, Prieto D, García-Pascual A (1993). NADPH-diaphorase and NANC relaxations are correlated in the sheep urinary tract. Neurosci Lett 163: 93–96.

Triguero D, Sancho M, García-Flores M, Garcia-Pascual A (2009). Presence of cyclic nucleotide-gated channels in the rat urethra and their involvement in nerve-mediated nitrergic relaxation. Am J Physiol Renal Physiol 297: F1353–F1360.

Ueno M, Sakamoto H, Kanenishi K, Onodera M, Akiguchi I, Hosokawa M (2001). Ultrastructural and permeability features of microvessels in the periventricular area of senescence-accelerated mice (SAM). Microsc Res Tech 53: 232–238.

Wagg A, Cohen M (2002). Medical therapy for the overactive bladder in the elderly. Age Ageing 31: 241–246.

Warburton AL, Santer RM (1994). Sympathetic and sensory innervations of the urinary tract in young adult and aged rats: a semi-quantitative histochemical and immunohistochemical study. Histochem J 26: 127–133.

Wuest M, Morgenstern K, Graf EM, Braeter M, Hakenberg OW, Wirth MP *et al*. (2005). Cholinergic and purinergic responses in isolated human detrusor in relation to age. J Urol 173: 2182–2189.

Yamamoto T, Ghosh R, de Groat WC, Somogyi T (2001). Facilitation of transmitter release in the urinary bladders of neonatal and adult rats via alpha1-adrenoceptors. Eur J Pharmacol 414: 31–35.

Yoshida M, Latifpour J, Nishimoto T, Weiss R (1991). Pharmacological characterization of alpha adrenergic receptors in the young and old female rabbit urethra. J Pharmacol Exp Ther 257: 1100–1108.

Yoshida M, Homma Y, Inadome A, Yono M, Seshita H, Miyamoto Y *et al*. (2001). Age-related changes in cholinergic and purinergic neurotransmission in human isolated bladder smooth muscles. Exp Gerontol 36: 99–109.

Yoshida M, Miyamae K, Iwashita H, Otani M, Inamode A (2004). Management of detrusor dysfunction in the elderly: changes in acetylcholine and adenosine triphosphate release during ageing. Urology 63 (Suppl 3A): 17–23.

Zhao W, Aboushwareb T, Turner C, Mathis C, Bennett C, Sonntag WE *et al*. (2010). Impaired bladder function in ageing male rats. J Urol 184: 378–385.